ALL SL_2-TILINGS COME FROM INFINITE TRIANGULATIONS

CHRISTINE BESSENRODT, THORSTEN HOLM, AND PETER JØRGENSEN

Abstract. An SL_2-tiling is a bi-infinite matrix of positive integers such that each adjacent 2×2-submatrix has determinant 1. Such tilings are infinite analogues of Conway–Coxeter friezes, and they have strong links to cluster algebras, combinatorics, mathematical physics, and representation theory.

We show that, by means of so-called Conway–Coxeter counting, every SL_2-tiling arises from a triangulation of the disc with two, three or four accumulation points.

This improves earlier results which only discovered SL_2-tilings with infinitely many entries equal to 1. Indeed, our methods show that there are large classes of tilings with only finitely many entries equal to 1, including a class of tilings with no 1's at all. In the latter case, we show that the minimal entry of a tiling is unique.

0. Introduction

A *Conway–Coxeter frieze of Dynkin type A_n* is an infinite strip of positive integers of the form shown in Figure 1. It consists of $n+2$ horizontal rows with an offset between odd and even rows. It is bordered by rows of ones and satisfies the condition $ad - bc = 1$ for each "diamond" $\begin{smallmatrix} & b & \\ a & & d \\ & c & \end{smallmatrix}$.

Conway–Coxeter friezes were introduced in [9] and [10] and inhabit a rich combinatorial theory. For instance, each frieze can be obtained by so-called *Conway–Coxeter counting* on a triangulation of the $(n+3)$-gon, see (28) and (29) in [9] and [10] or Definition 2.1 below.

$$\begin{array}{ccccccccccccccccccc}
\cdots & 1 & & 1 & & 1 & & 1 & & 1 & & 1 & & 1 & & 1 & \\
& 2 & & 1 & & 3 & & 2 & & 2 & & 1 & & 4 & & 2 & & 1 & \cdots \\
\cdots & 1 & & 2 & & 5 & & 3 & & 1 & & 3 & & 7 & & 1 & & 2 & \\
& 3 & & 1 & & 3 & & 7 & & 1 & & 2 & & 5 & & 3 & & 1 & \cdots \\
\cdots & 2 & & 1 & & 4 & & 2 & & 1 & & 3 & & 2 & & 2 & & 1 & \\
& 1 & & 1 & & 1 & & 1 & & 1 & & 1 & & 1 & & 1 & & 1 & \cdots
\end{array}$$

Figure 1. A Conway-Coxeter frieze of Dynkin type A_4.

2010 *Mathematics Subject Classification.* 05E15, 13F60.

Key words and phrases. Arc, disc with accumulation points, Conway–Coxeter frieze, Igusa–Todorov cluster category, Ptolemy formula, tiling, triangulation.

SL_2-*tilings* are infinite analogues of Conway–Coxeter friezes. They are bi-infinite matrices of positive integers such that each adjacent 2×2-submatrix has determinant 1, see Figure 3. They were introduced by Assem, Reutenauer, and Smith in [3] and have turned out to be important objects with a wealth of connections to cluster algebras, combinatorics, mathematical physics, and representation theory.

Some classes of SL_2-tilings were discovered in [3] and [18], but there were examples not belonging to the classes, see [18, exa. 2.9], and there was no insight into the structure of the set of all SL_2-tilings.

We improve the results from [3] and [18] significantly by showing that every SL_2-tiling can be obtained by Conway–Coxeter counting on an *infinite triangulation of the disc with two, three, or four accumulation points*. We also show that the SL_2-tilings found in [3] and [18] are rather special, because they have infinitely many entries equal to 1. Our methods reveal that there are large classes of SL_2-tilings with only finitely many 1's, and even a class of tilings with no 1's at all, see Remark 3.10.

In the latter case, we show that the minimal entry of a tiling is unique, see Lemma 12.4.

Motivations for studying SL_2-tilings. The introduction of SL_2-tilings in [3] was motivated by applications to linear recurrence relations for certain friezes, and to formulae for cluster variables in Euclidean type, see [3, secs. 7 and 8]. There is an application by Assem and Reutenauer in [2] to formulae for cluster seeds in types A and $\tilde{A}$.

SL_2-tilings were applied to the theory of cluster characters by Assem, Dupont, Schiffler, and Smith in [1] and Jørgensen and Palu in [20]. Cluster characters were introduced by Palu in [23] to formalise cluster categorification.

Di Francesco in [11], [12] and Di Francesco and Kedem in [13], [14] showed how SL_2-tilings are linked to mathematical physics, where a so-called T-system of type A_1 is simply a pair of SL_2-tilings, albeit with Laurent polynomial values.

SL_2-tilings were generalised by Bergeron and Reutenauer in [5] to SL_k-tilings. Other types of SL_2-tilings, relaxing parts of the definition, were obtained by Baur, Parsons, and Tschabold in [4], Morier-Genoud, Ovsienko, and Tabachnikov in [22], Tschabold in [24], and also in [18] and [20].

We continue with a more detailed explanation of this paper.

Primer on Conway–Coxeter counting. Figure 2 shows a triangulation $\mathfrak{T}$ of the disc with two accumulation points, D_2. The notches indicate marked points on the boundary of the disc, also called *vertices*. There are countably many vertices in each of two *intervals* given by the upper and lower half circles. The vertices converge clockwise and anticlockwise to two *accumulation points* marked with small circles. A numbering of the vertices is shown in black; the superscripts I and III are not powers but distinguish between the vertices on the two intervals. The triangulation $\mathfrak{T}$ is a set of arcs between non-neighbouring vertices which divides the disc into triangular regions. The figure shows only a finite part of the infinite set $\mathfrak{T}$.

Conway–Coxeter counting on $\mathfrak{T}$ is the following procedure: Start with a fixed vertex μ and label it 0. If vertex ν is a neighbour of μ, or linked to μ by an arc in $\mathfrak{T}$, then ν is labelled 1. Now iterate the following: If a triangular region defined by $\mathfrak{T}$ has precisely two labelled vertices π and ρ with labels i and j, then its third vertex σ is labelled $i + j$. The label which

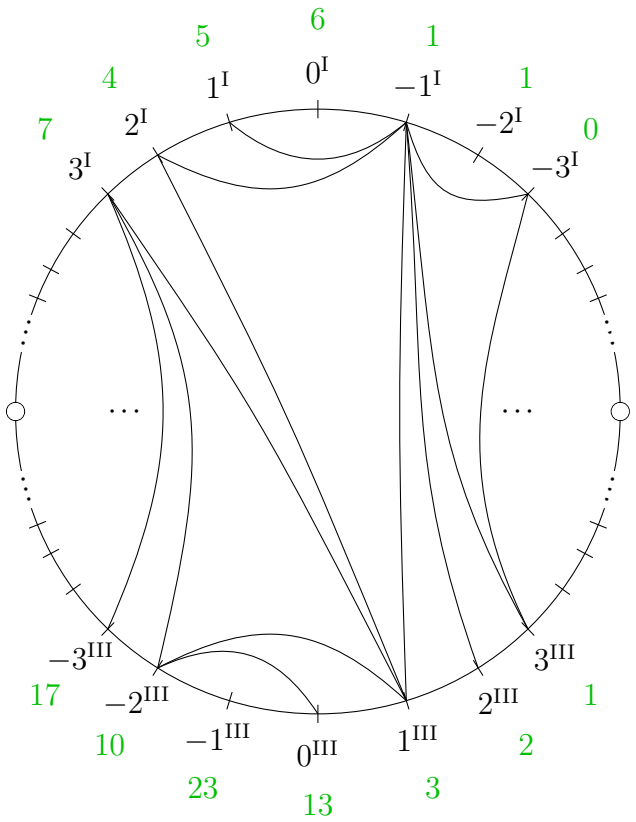

FIGURE 2. A triangulation $\mathfrak{T}$ of the disc with two accumulation points, D_2. Black numbers label the vertices, green numbers show an example of Conway–Coxeter counting starting at vertex -3^{I}.

eventually appears at σ is denoted $\mathfrak{T}(\mu, \sigma)$. The green numbers in Figure 2 show $\mathfrak{T}(\mu, \sigma)$ for $\mu = -3^{\mathrm{I}}$.

It follows from results by Conway and Coxeter that

$$t(b, v) = \mathfrak{T}(b^{\mathrm{I}}, v^{\mathrm{III}}) \tag{0.1}$$

with $b, v \in \mathbb{Z}$ defines an SL$_2$-tiling t, said to *arise from* $\mathfrak{T}$ *by Conway–Coxeter counting*. Part of t is shown on the left in Figure 3. Note that we use matrix notation so b increases when going down, v increases when going right.

SL$_2$-tilings without 1's and the main result. Not every SL$_2$-tiling can be obtained as above. To see so, observe that if $\mathfrak{T}$ contains an arc between a vertex b^{I} on the top half circle and a vertex v^{III} on the bottom half circle, then $\mathfrak{T}(b^{\mathrm{I}}, v^{\mathrm{III}}) = 1$ so t has at least one entry equal to 1. But the right half of Figure 3 shows part of an SL$_2$-tiling t' with no entry equal to 1. One could try to obtain t' by letting $\mathfrak{T}$ have no arcs between the top half circle and the bottom half circle, but this will not work: If there are no such connecting arcs, then Conway–Coxeter counting does not terminate. Indeed, the procedure never reaches the bottom half circle at all, so no labels are defined there.

Figure 4 shows a more sophisticated triangulation $\mathfrak{T}'$ of the disc with four accumulation points. There are now vertices in four intervals, converging clockwise and anticlockwise

$$
\begin{array}{ccccccccc}
 & & & \vdots & & & & & \\
 & 17 & 10 & 23 & 13 & 3 & 2 & 1 & \\
 & 22 & 13 & 30 & 17 & 4 & 3 & 2 & \\
 & 5 & 3 & 7 & 4 & 1 & 1 & 1 & \\
\cdots & 13 & 8 & 19 & 11 & 3 & 4 & 5 & \cdots \\
 & 8 & 5 & 12 & 7 & 2 & 3 & 4 & \\
 & 3 & 2 & 5 & 3 & 1 & 2 & 3 & \\
 & 1 & 1 & 3 & 2 & 1 & 3 & 5 & \\
 & & & \vdots & & & & &
\end{array}
\qquad
\begin{array}{ccccccccc}
 & & & \vdots & & & & & \\
 & 25 & 18 & 11 & 4 & 9 & 5 & 11 & \\
 & 18 & 13 & 8 & 3 & 7 & 4 & 9 & \\
 & 29 & 21 & 13 & 5 & 12 & 7 & 16 & \\
\cdots & 11 & 8 & 5 & 2 & 5 & 3 & 7 & \cdots \\
 & 15 & 11 & 7 & 3 & 8 & 5 & 12 & \\
 & 34 & 25 & 16 & 7 & 19 & 12 & 29 & \\
 & 87 & 64 & 41 & 18 & 49 & 31 & 75 & \\
 & & & \vdots & & & & &
\end{array}
$$

FIGURE 3. Left: The SL_2-tiling t obtained by Conway–Coxeter counting on $\mathfrak{T}$ from Figure 2. Right: An SL_2-tiling t' with no entry equal to 1.

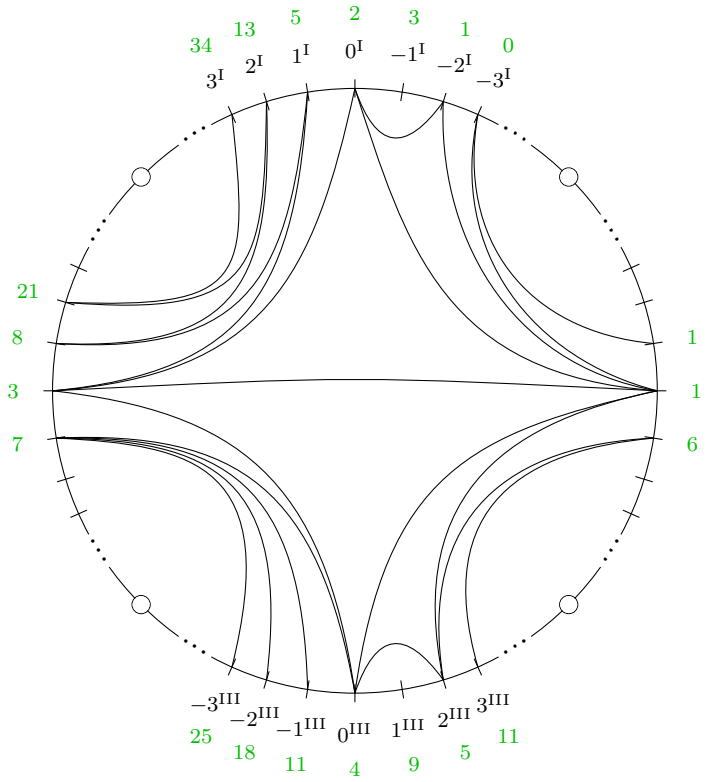

FIGURE 4. A triangulation $\mathfrak{T}'$ of the disc with four accumulation points, D_4. Black numbers label the vertices, green numbers show an example of Conway–Coxeter counting starting at vertex -3^{I}.

to four accumulation points marked with small circles. The top and bottom intervals are numbered I and III as above; indeed, two of the intervals on a disc will always be numbered I and III regardless of how many accumulation points there are. A numbering of the vertices in the top and bottom intervals is shown in black, and green numbers show the $\mathfrak{T}'(\mu, \sigma)$ for

$$\begin{array}{ccccccccccc}
\ddots & & & & & \vdots & & & & & \\
 & 0 & 1 & 1 & 6 & 5 & 4 & 7 & & & \\
 & & 0 & 1 & 7 & 6 & 5 & 9 & & & \\
 & & & 0 & 1 & 1 & 1 & 2 & \cdots & & \\
 & & & & 0 & 1 & 2 & 5 & & & \\
 & & & & & 0 & 1 & 3 & & & \\
 & & & & & & 0 & 1 & & & \\
 & & & & & & & 0 & & & \\
 & & & & & & & & \ddots & &
\end{array}$$

FIGURE 5. An infinite frieze.

$\mu = -3^{\mathrm{I}}$. The SL_2-tiling arising from $\mathfrak{T}'$ by Conway–Coxeter counting is defined as above: $t'(b, v) = \mathfrak{T}'(b^{\mathrm{I}}, v^{\mathrm{III}})$, and this is in fact the t' in the right half of Figure 3.

The extra accumulation points mean that there is room in $\mathfrak{T}'$ for a horizontal arc which blocks $\mathfrak{T}'$ from having arcs between the top and bottom intervals. This means that $\mathfrak{T}'(b^{\mathrm{I}}, v^{\mathrm{III}})$ is never equal to 1, so t' has no entry equal to 1. Note that in this example, Conway–Coxeter counting does indeed terminate with labels on the bottom interval because it can progress through the side intervals.

Our main result is that four accumulation points are sufficient for every SL_2-tiling to arise:

Theorem A. *Let t be an SL_2-tiling. There exists a good triangulation $\mathfrak{T}$ of the disc with two, three, or four accumulation points, such that t arises from $\mathfrak{T}$ by Conway–Coxeter counting between two of the intervals which go from one accumulation point to the next.* □

The notion of a *good triangulation* is made precise in Definition 1.9. The point is that Conway–Coxeter counting always terminates for these. Theorem A is a portmanteau of Theorems 6.1, 7.4, 8.2, 9.4, 10.2, and 13.8, each of which starts with an SL_2-tiling t of a certain type and constructs a good triangulation $\mathfrak{T}$.

On the proof of Theorem A. The construction of $\mathfrak{T}$ is split across six theorems because the details depend strongly on t; specifically, on the pattern of entries equal to 1. However, the philosophy is the same in all cases as we now explain.

Let t be an SL_2-tiling. On the one hand, t gives rise to two *infinite friezes* in the sense of Tschabold, see [24, def. 1.1] or Definition 3.1 and Figure 5. They are defined by

$$p(a,d) = \begin{vmatrix} t(a,w) & t(a,w+1) \\ t(d,w) & t(d,w+1) \end{vmatrix} \quad , \quad q(u,x) = \begin{vmatrix} t(c,u) & t(c,x) \\ t(c+1,u) & t(c+1,x) \end{vmatrix}$$

for integers $a \leqslant d$, $u \leqslant x$. Note that the integers w and c can be chosen freely; $p(a,d)$ and $q(u,x)$ do not depend on them. To say that p is an infinite frieze means that $p(a,a) = 0$, $p(a,a+1) = 1$, $p(a,d) \geqslant 1$ for $a < d$, and, when writing p as a matrix, each 2×2-submatrix which makes sense has determinant 1. Note that to improve the compatibility with SL_2-tilings, our convention for indexing an infinite frieze differs from [24, def. 1.1].

On the other hand, a putative good triangulation $\mathfrak{T}$ gives rise not merely to the SL_2-tiling of Equation (0.1), but also to two infinite friezes defined by

$$(a, d) \mapsto \mathfrak{T}(a^{\mathrm{I}}, d^{\mathrm{I}}) \quad , \quad (u, x) \mapsto \mathfrak{T}(u^{\mathrm{III}}, x^{\mathrm{III}})$$

for integers $a \leqslant d$, $u \leqslant x$; this again follows from results by Conway and Coxeter.

To prove Theorem A we must show that when t is an SL_2-tiling, there is a good triangulation $\mathfrak{T}$ satisfying Equation (0.1). However, we will tackle the seemingly harder problem of also asking for

$$p(a, d) = \mathfrak{T}(a^{\mathrm{I}}, d^{\mathrm{I}}), \tag{0.2}$$

$$q(u, x) = \mathfrak{T}(u^{\mathrm{III}}, x^{\mathrm{III}}) \tag{0.3}$$

for $a \leqslant d$, $u \leqslant x$. This actually turns out to be easier because the entries in the triple (t, p, q) and the numbers $\mathfrak{T}(\mu, \nu)$ satisfy two strong sets of equations called *Ptolemy relations* which we do not list here, but see Lemmas 2.3(v) and 3.3. They mean that, when $\mathfrak{T}$ has been constructed, in order to prove Equations (0.1) through (0.3) in general, it is sufficient to do so in a relatively small set of special cases.

For example, suppose that t has infinitely many entries equal to 1 in both the first and the third quadrant; this is the case considered in Theorem 6.1. For such a t, we will show that the set of arcs

$$\begin{aligned}\Theta(t) = \big\{ \{b^{\mathrm{I}}, v^{\mathrm{III}}\} \,\big|\, t(b, v) = 1 \big\} \cup \big\{ \{a^{\mathrm{I}}, d^{\mathrm{I}}\} \,\big|\, a + 2 \leqslant d,\, p(a, d) = 1 \big\} \\ \cup \big\{ \{u^{\mathrm{III}}, x^{\mathrm{III}}\} \,\big|\, u + 2 \leqslant x,\, q(u, x) = 1 \big\}\end{aligned} \tag{0.4}$$

is a good triangulation of D_2 (observe that we think of an arc as a purely combinatorial object specified by giving the end vertices). Moreover, if we set $\mathfrak{T} = \Theta(t)$ then Equations (0.1) through (0.3) hold in some special cases: If $t(b, v) = 1$ then $\{b^{\mathrm{I}}, v^{\mathrm{III}}\} \in \mathfrak{T}$ whence $\mathfrak{T}(b^{\mathrm{I}}, v^{\mathrm{III}}) = 1$, so Equation (0.1) holds. Likewise, if $p(a, d) = 1$ then Equation (0.2) holds, and if $q(u, x) = 1$ then Equation (0.3) holds. Using only this, the Ptolemy relations turn out to imply the three equations in general. In particular, Equation (0.1) holds in general, so t arises from $\mathfrak{T}$ by Conway–Coxeter counting.

Before ending this discussion, let us highlight another useful phenomenon: The special cases $d = a + 2$ of Equation (0.2) and (symmetrically) $x = u + 2$ of Equation (0.3) imply the two equations in general. Indeed, this is just the easy fact that the second diagonal, or *quiddity sequence*, of an infinite frieze determines the whole frieze, see [24, rmk. 1.3]. When t is given, it is hence important to be able to construct a good triangulation $\mathfrak{T}$ which satisfies Equations (0.2) and (0.3) in these special cases. We will use the following approach: The vertices a^{I}, $(a+1)^{\mathrm{I}}$, $(a+2)^{\mathrm{I}}$ are consecutive on the disc. It is known that hence, if $\mathfrak{T}$ can be constructed, then

$$\mathfrak{T}\big(a^{\mathrm{I}}, (a+2)^{\mathrm{I}}\big) = 1 + \big(\text{the number of arcs in } \mathfrak{T} \text{ which end at } (a+1)^{\mathrm{I}}\big).$$

To get Equation (0.2) for $d = a + 2$, we must construct $\mathfrak{T}$ such that

$$p(a, a+2) = 1 + \big(\text{the number of arcs in } \mathfrak{T} \text{ which end at } (a+1)^{\mathrm{I}}\big).$$

In Theorems 7.4, 8.2, 9.4, 10.2, and 13.8, this is accomplished by starting with the set of arcs $\Theta(t)$ from Equation (0.4) and adding arcs so that, eventually, there are $p(a, a+2) - 1$ arcs ending at $(a+1)^{\mathrm{I}}$ for each a. See for instance Figure 21 where the arcs in $\Theta(t)$ are black and the additional arcs are red. The figure also illustrates that the additional arcs need somewhere to end. This is the reason we need more intervals than I and III. The number of arcs to be added at $(a+1)^{\mathrm{I}}$ is given by the *defect* $\mathrm{def}_p(a+1)$ introduced in Definition 5.4;

this is the rationale for defining and manipulating defects in Section 5. See also Figure 21 and its caption.

Link to the cluster categories of Igusa and Todorov. Let n be 2, 3, or 4, and let D_n be the disc with n accumulation points. The set of vertices of D_n is an example of a cyclic poset in the sense of Igusa and Todorov, see [19, def. 1.1.12]. There is an associated cluster category $\mathscr{C}$ with infinite clusters, see [19, thm. 2.4.1]. It categorifies D_n in the sense that there is a bijection between arcs in D_n and indecomposable objects in $\mathscr{C}$, such that crossing of arcs corresponds to existence of non-split extensions. Moreover, if $\mathfrak{T}$ is a good triangulation of D_n, then the arcs in $\mathfrak{T}$ correspond to a set of indecomposable objects whose finite direct sums form a cluster tilting subcategory $\mathscr{T}$ of $\mathscr{C}$. See [16] for more details.

There is an arithmetic Caldero–Chapoton map $\rho_{\mathscr{T}}$ associated to $\mathscr{C}$ and $\mathscr{T}$. As indicated by the name, the map is due to Caldero and Chapoton, but the specific version we have in mind is the one from [18, def. 3.1]. It is a map

$$\varphi_{\mathscr{T}} : \operatorname{obj} \mathscr{C} \to \mathbb{Z}$$

which can be computed by Conway–Coxeter counting; this follows from [20, prop. 1.10] by the method used to prove [17, thm. 5.4]. Hence if $a_{\mu\nu}$ in $\mathscr{C}$ is the indecomposable object corresponding to the arc $\{\mu, \nu\}$, then

$$\varphi_{\mathscr{T}}(a_{\mu\nu}) = \mathfrak{T}(\mu, \nu).$$

This means that we can view $\mathscr{C}$ and $\varphi_{\mathscr{T}}$ as categorifying the SL_2-tiling arising from $\mathfrak{T}$ by Conway–Coxeter counting.

This is of interest because there is a more general Caldero–Chapoton map

$$\rho_{\mathscr{T}} : \operatorname{obj} \mathscr{C} \to \mathbb{Q}(x_t \,|\, t \text{ indecomposable in } \mathscr{T})$$

with Laurent polynomial values whose image generates a cluster algebra with infinite clusters, see [20, thm. 2.3 and cor. 2.5]. The SL_2-tiling arising from $\mathfrak{T}$ by Conway–Coxeter counting can be recovered by specialising the initial cluster variables x_t to 1. Such cluster algebras have so far only been studied carefully for the disc with one accumulation point. They have several interesting properties different from cluster algebras with finite clusters, and seem likely to be of interest also for larger numbers of accumulation points. See [15] by Grabowski and Gratz.

Structure of the paper. Theorem A will not be proved in one go, but sums up Theorems 6.1, 7.4, 8.2, 9.4, 10.2, and 13.8. Each of these starts with an SL_2-tiling t with a certain pattern of entries equal to 1 and constructs a triangulation $\mathfrak{T}$ of the disc with two, three, or four accumulation points.

Reading the theorems in order will make it clear that they cover every possible SL_2-tiling t: They progress through SL_2-tilings t with fewer and fewer entries equal to 1, ending with no 1's at all in Theorem 13.8.

Conversely, SL_2-tilings of the types described in the theorems do exist: In each case, they can be obtained as the SL_2-tilings arising by Conway–Coxeter counting from triangulations of the type constructed in the theorem, see Remark 3.10.

Section 1 gives formal definitions relating to triangulations of the disc with accumulation points. Section 2 recalls some properties of Conway–Coxeter counting. Section 3 shows some results on SL_2-tilings and their associated infinite friezes. Section 4 starts with an SL_2-tiling t

and constructs a partial triangulation $\Theta(t)$. In each subsequent case, the (full) triangulation $\mathfrak{T}$ is obtained either as $\Theta(t)$ itself (Theorem 6.1), or is constructed by adding arcs to $\Theta(t)$ (Theorems 7.4, 8.2, 9.4, 10.2, and 13.8). Section 5 introduces what we call defects and shows some properties. The defects provide information about how many arcs we must add to $\Theta(t)$ to get $\mathfrak{T}$.

Sections 6 through 10 prove Theorems 6.1, 7.4, 8.2, 9.4, 10.2. Section 11 shows a technical result on Conway–Coxeter friezes, Section 12 shows that an SL_2-tiling with no entry equal to 1 has a unique minimum, and Section 13 proves Theorem 13.8, thereby completing the proof of Theorem A.

1. Triangulations of the disc with accumulation points and other basic definitions

Setup 1.1. Throughout, C is a circle with anticlockwise orientation, D is a disc with boundary C, and n is 2, 3, or 4.

Notation 1.2. Let $\mu_1, \ldots, \mu_m$ be points on C.

The string of inequalities $\mu_1 < \cdots < \mu_m$ will mean that each μ_i is different from its predecessor, and that if we start from μ_1 and move anticlockwise on C by one full turn, then we encounter the points in precisely the order $\mu_1, \ldots, \mu_m$.

It is straightforward to modify this to permit the inequality sign $\leqslant$ as well as infinite strings of inequalities.

Definition 1.3 (The disc with four accumulation points)**.** Let D_4, the *disc with four accumulation points*, be the object sketched in Figure 6.

More formally, D_4 is the disc D along with four points $\xi_{\mathrm{I}} < \xi_{\mathrm{II}} < \xi_{\mathrm{III}} < \xi_{\mathrm{IV}}$ on the boundary C called *accumulation points of* D_4, and infinitely many points on C called *vertices of* D_4, defined as follows:

For each $\mathrm{J} \in \{\mathrm{I}, \mathrm{II}, \mathrm{III}, \mathrm{IV}\}$, let $\ldots, -1^{\mathrm{J}}, 0^{\mathrm{J}}, 1^{\mathrm{J}}, \ldots$ be countably many points on C which satisfy:

- $\xi_{\mathrm{J}-1} < \cdots < -1^{\mathrm{J}} < 0^{\mathrm{J}} < 1^{\mathrm{J}} < \cdots < \xi_{\mathrm{J}}$,
- the sequence $0^{\mathrm{J}}, 1^{\mathrm{J}}, 2^{\mathrm{J}}, \ldots$ converges to ξ_{J},
- the sequence $0^{\mathrm{J}}, -1^{\mathrm{J}}, -2^{\mathrm{J}}, \ldots$ converges to $\xi_{\mathrm{J}-1}$.

Here $\mathrm{J} - 1$ stands for the Roman numeral one below J, or IV if $\mathrm{J} = \mathrm{I}$. The vertices of D_4 are the points $\ldots, -1^{\mathrm{J}}, 0^{\mathrm{J}}, 1^{\mathrm{J}}, \ldots$ for $\mathrm{J} \in \{\mathrm{I}, \mathrm{II}, \mathrm{III}, \mathrm{IV}\}$.

The set

$$\{\omega \in C \mid \xi_{\mathrm{J}-1} < \omega < \xi_{\mathrm{J}}\}$$

will be called *interval* J *of the boundary of* D_4. There is an obvious notion of when two intervals are *neighbouring*.

Our convention for numbering the intervals of the boundary of D_4 is shown in simplified form in Figure 7.

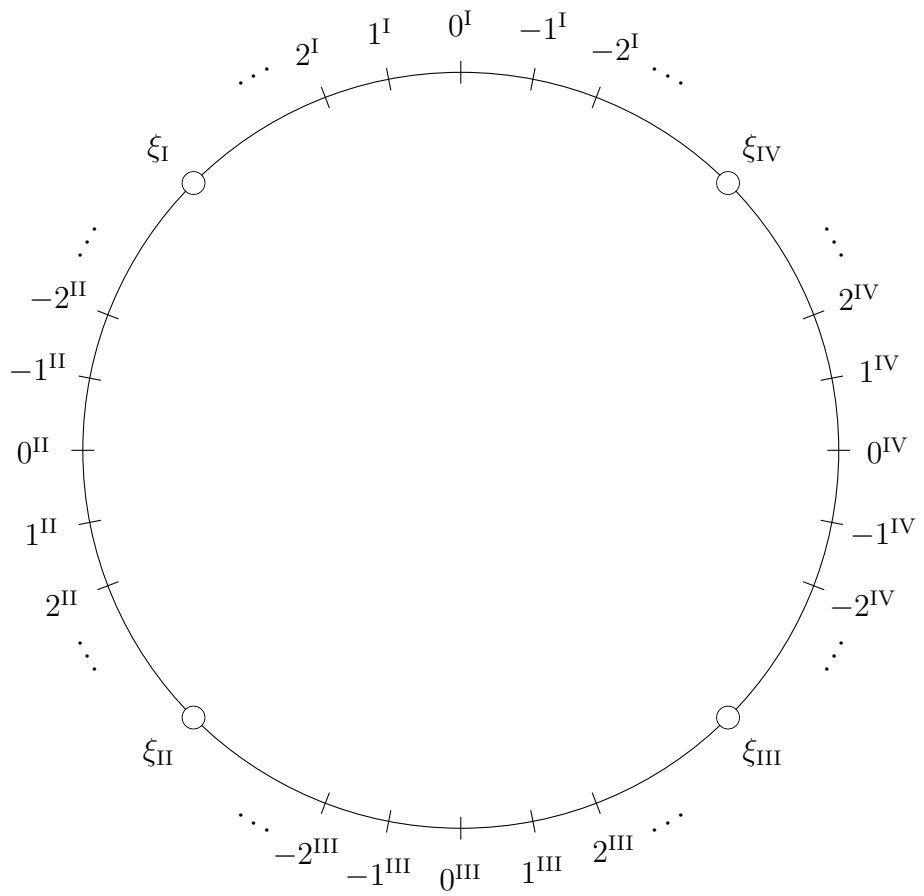

FIGURE 6. This is D_4, the disc with four accumulation points, ξ_{I} through ξ_{IV}.

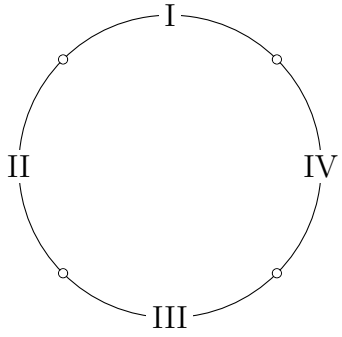

FIGURE 7. A simpler view of the disc with four accumulation points, D_4, and our convention for numbering the intervals of the boundary.

Definition 1.4 (The disc with two or three accumulation points)**.** We can mimic Definition 1.3 in order to define D_2, the disc with two accumulation points, and D_3, the disc with three accumulation points. For reasons which will be explained later, in case of D_2 we will denote the intervals by Roman numerals I and III, and in case of D_3 by Roman numerals $\{\mathrm{I}, \mathrm{II}, \mathrm{III}\}$ or $\{\mathrm{I}, \mathrm{III}, \mathrm{IV}\}$.

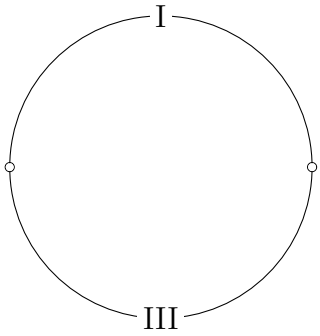

FIGURE 8. The disc with two accumulation points, D_2, and our convention for numbering the intervals of the boundary.

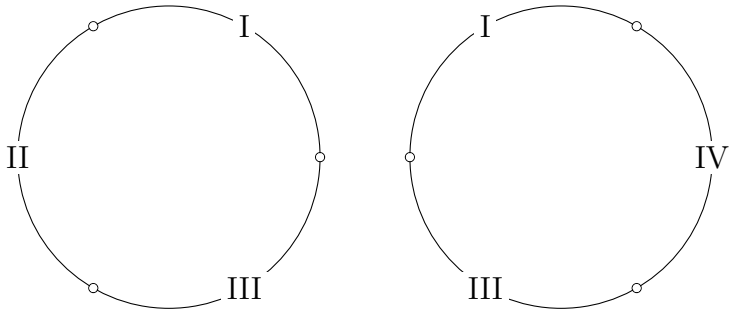

FIGURE 9. The disc with three accumulation points, D_3, and our two possible conventions for numbering the intervals of the boundary.

That is, intervals I and III are always present, but II and/or IV may be dropped; see Figures 8 and 9.

Notation 1.5. Recall that n is 2, 3 or 4, so we may consider D_n, the disc with n accumulation points.

Generic integers will often be denoted by i, j, k, ℓ, m and generic vertices of D_n often by ι, κ, μ, ν, π, ρ, σ.

If J is an interval of the boundary of D_n and m is an integer, then the vertex m^{J} is in J. Depending on whether J is I, II, III, or IV, we will typically replace m by one of the letters in Figure 10.

In subsequent figures, the superscripts of vertices will be omitted since it is clear from a figure when two vertices belong to different intervals. Superscripts will, however, be used in the main text.

Definition 1.6 (Edges, arcs, and crossing)**.** Let μ be a vertex of D_n. There are evident notions of the *previous* vertex μ^- and the *next* vertex μ^+. These are called the *neighbouring* vertices of μ.

When μ and ν are different vertices of D_n, we can consider the set $\{\mu, \nu\}$. If μ and ν are neighbouring vertices then $\{\mu, \nu\}$ is called the *edge between μ and ν in D_n*, and if μ and ν are non-neighbouring vertices then $\{\mu, \nu\}$ is called the *arc between μ and ν in D_n*. In either case, we say that $\{\mu, \nu\}$ *ends at μ and ν* and *links these two vertices*.

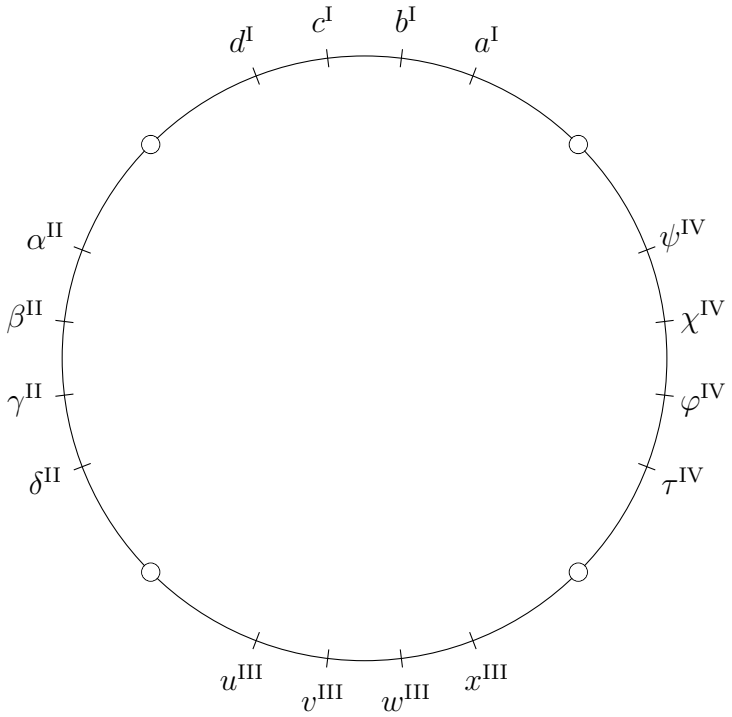

FIGURE 10. Depending on the interval, we typically use these labels for the vertices.

This is a combinatorial definition, but we keep in mind the geometrical intuition to think of an edge as part of the circle C bounding the disc D, and of an arc as an actual arc inside D.

The arcs $\{\mu, \nu\}$ and $\{\pi, \rho\}$ are said to *cross* if $\mu < \pi < \nu < \rho$ or $\pi < \mu < \rho < \nu$. This is compatible in an evident way with the geometrical intuition of the previous paragraph, see Figure 14.

Definition 1.7 (Internal, connecting, clockwise, and anticlockwise arcs)**.** An arc $\{\mu, \nu\}$ is called *internal* if μ and ν belong to the same interval. Otherwise it is called *connecting* (because it connects two different intervals). Note that the words *peripheral* and *bridging* are used in essentially the same sense in [4] and [24].

If $\{\mu, \nu\}$ is an internal arc or an edge, then either $\nu = \mu^{+ + \cdots +}$ or $\nu = \mu^{- - \cdots -}$. In the former case, we say that $\{\mu, \nu\}$ *goes anticlockwise from* μ, in the latter case that $\{\mu, \nu\}$ *goes clockwise from* μ.

Definition 1.8 (Blocking an accumulation point)**.** Let J and K be neighbouring intervals of the boundary of D_n separated by the accumulation point ξ, such that if $\iota \in \mathrm{J}$ and $\kappa \in \mathrm{K}$ are vertices then $\iota < \xi < \kappa$.

Let $\mathfrak{T}$ be a set of arcs in D_n. We say that $\mathfrak{T}$ *blocks the accumulation point* ξ if it contains the configuration shown in Figure 11.

More formally, $\mathfrak{T}$ must contain arcs $\{\iota_i, \kappa_i\}$ for $i \geqslant 1$ where the vertices $\iota_i \in \mathrm{J}$ and $\kappa_i \in \mathrm{K}$ satisfy $\iota_1 < \iota_2 < \cdots < \xi < \cdots < \kappa_2 < \kappa_1$. Note that the ι_i and the κ_i converge to ξ from opposite sides.

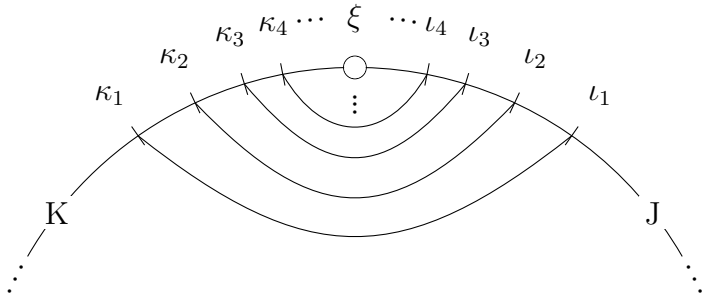

FIGURE 11. The arcs block the accumulation point ξ.

Definition 1.9 (Triangulations)**.** A set of pairwise non-crossing arcs in D_n is called a *partial triangulation of* D_n, and a maximal set of pairwise non-crossing arcs in D_n is called a *triangulation of* D_n.

A partial triangulation $\mathfrak{T}$ of D_n is called *good* if it blocks each accumulation point of D_n. It is called *locally finite* if, for each vertex μ of D_n, only finitely many arcs in $\mathfrak{T}$ end at μ.

Definition 1.10 (Vertex sets compatible with a partial triangulation)**.** Let $\mathfrak{T}$ be a partial triangulation of D_n. A finite set of $m \geqslant 2$ vertices $\mu_1 < \mu_2 < \cdots < \mu_m$ of D_n is said to be *compatible with* $\mathfrak{T}$ if each pair $\{\mu_1, \mu_2\}$, $\{\mu_2, \mu_3\}$, …, $\{\mu_m, \mu_1\}$ is either an edge or an arc in $\mathfrak{T}$.

The pairs $\{\mu_1, \mu_2\}$, $\{\mu_2, \mu_3\}$, …, $\{\mu_m, \mu_1\}$ can be viewed as the edges of a finite polygon P with vertices equal to the μ_i, and we say that the set $M = \{\mu_1, \ldots, \mu_m\}$ *spans* P.

The remaining arcs in $\mathfrak{T}$ between the μ_i form a partial triangulation $\mathfrak{T}_P$ of P, and we say that $\mathfrak{T}$ *restricts to* $\mathfrak{T}_P$. If $\mathfrak{T}$ is a triangulation of D_n then $\mathfrak{T}_P$ is a triangulation of P.

The following special cases will play a prominent role.

(i) Let J be an interval of the boundary of D_n. If $a < d$ are such that $\{a^{\mathrm{J}}, d^{\mathrm{J}}\} \in \mathfrak{T}$ or $\{a^{\mathrm{J}}, d^{\mathrm{J}}\}$ is an edge, then the set of vertices $\{a^{\mathrm{J}}, \ldots, d^{\mathrm{J}}\}$ is compatible with $\mathfrak{T}$ and spans a finite polygon P called *the polygon below* $\{a^{\mathrm{J}}, d^{\mathrm{J}}\}$. See the left part of Figure 12 where $n = 4$ and J = I.

(ii) Let J and K be distinct intervals of the boundary of D_n. If $a \leqslant d$ and $u \leqslant x$ are such that $\{a^{\mathrm{J}}, x^{\mathrm{K}}\}, \{d^{\mathrm{J}}, u^{\mathrm{K}}\} \in \mathfrak{T}$ then the set of vertices $a^{\mathrm{J}}, \ldots, d^{\mathrm{J}}, u^{\mathrm{K}}, \ldots, x^{\mathrm{K}}$ is compatible with $\mathfrak{T}$ and spans a finite polygon R called *the polygon between* $\{a^{\mathrm{J}}, x^{\mathrm{K}}\}$ *and* $\{d^{\mathrm{J}}, u^{\mathrm{K}}\}$. See the right part of Figure 12 where $n = 4$, J = I, K = III.

Lemma 1.11. *Let $\mathfrak{T}$ be a good triangulation of D_n and let N be a finite set of vertices of D_n. Then there exists a finite set M of vertices such that $N \subseteq M$ and M is compatible with $\mathfrak{T}$.*

The set M spans a finite polygon P, and $\mathfrak{T}$ restricts to a triangulation $\mathfrak{T}_P$ of P.

Proof. Consider the following construction of a set M of vertices compatible with $\mathfrak{T}$:

Start by including in M a vertex in interval I. Move anticlockwise around D_n and include in M the vertices in interval I encountered. End with a vertex linked to interval II by an arc in $\mathfrak{T}$.

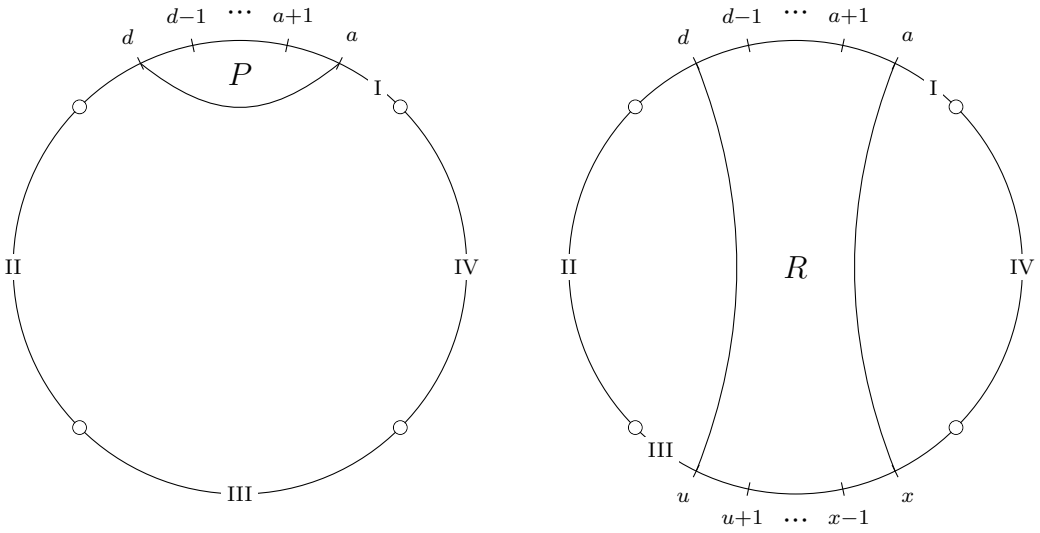

FIGURE 12. There is a finite polygon P below the arc $\{a^{\mathrm{I}}, d^{\mathrm{I}}\}$. The vertices of P are a^{I}, $(a+1)^{\mathrm{I}}$, …, $(d-1)^{\mathrm{I}}$, d^{I}. Among them, $(a+1)^{\mathrm{I}}$, $(a+2)^{\mathrm{I}}$, …, $(d-2)^{\mathrm{I}}$, $(d-1)^{\mathrm{I}}$ are said to be strictly below $\{a^{\mathrm{I}}, d^{\mathrm{I}}\}$. There is similar terminology for the finite polygon R, see Definitions 1.10 and 5.1.

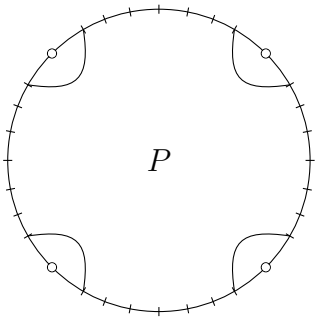

FIGURE 13. The four arcs are elements of a good triangulation $\mathfrak{T}$ of D_4, so the set M of vertices shown in the figure is compatible with $\mathfrak{T}$. The set M spans a finite polygon P. The four arcs can be viewed as four of the edges of P, and $\mathfrak{T}$ restricts to a triangulation $\mathfrak{T}_P$ of P.

Continue by including in M the vertex at the other end of this arc. Move anticlockwise around D_n and include in M the vertices in interval II encountered. End with a vertex linked to interval III by an arc in $\mathfrak{T}$.

Continue in the same fashion, thereby defining a set of vertices M as shown in Figure 13. The set M spans a finite polygon P and $\mathfrak{T}$ restricts to a triangulation $\mathfrak{T}_P$ of P; see Definition 1.10.

This proves the lemma since we can always accomplish $N \subseteq M$ by making M sufficiently big. Namely, N is finite, and the arcs which link different intervals in the construction of M can be chosen arbitrarily close to the accumulation points because $\mathfrak{T}$ is good. □

2. Conway–Coxeter counting

Definition 2.1 (Conway–Coxeter counting)**.** Let P be a finite polygon with a triangulation $\mathfrak{S}$ and fix a vertex μ of P. The following procedure is due to [10, (32)], see also [7, sec. 2]. We will refer to it as *Conway–Coxeter counting*:

Each vertex of P is assigned a non-negative integer by the following inductive procedure. The vertex μ is assigned 0. If $\{\mu, \nu\}$ is an edge or an arc in $\mathfrak{S}$, then the vertex ν is assigned 1. If there is a triangle in $\mathfrak{S}$ of which only two vertices, say π and ρ, have been assigned integers, say a and b, then the third vertex is assigned $a + b$.

We let $\mathfrak{S}(\mu, \nu)$ denote the integer assigned to vertex ν.

Remark 2.2. Let $\mathfrak{T}$ be a good triangulation of D_n and let μ, ν be vertices of D_n.

By Lemma 1.11, we can pick a finite set of vertices M such that $\mu, \nu \in M$ and such that M is compatible with $\mathfrak{T}$ in the sense of Definition 1.10. The set M spans a finite polygon P, and $\mathfrak{T}$ restricts to a triangulation $\mathfrak{T}_P$ of P, so Conway–Coxeter counting defines a non-negative integer $\mathfrak{T}_P(\mu, \nu)$.

It is easy to see that $\mathfrak{T}_P(\mu, \nu)$ does not depend on the choice of vertex set M. Indeed, $\mathfrak{T}_P(\mu, \nu)$ can be computed by following the inductive procedure of Definition 2.1 on $\mathfrak{T}$ itself. Accordingly, we drop the subscript P and write $\mathfrak{T}(\mu, \nu)$.

Lemma 2.3 (Basic properties of Conway–Coxeter counting)**.** *Let $\mathfrak{T}$ be a triangulation of a finite polygon P or a good triangulation of D_n. Then Conway–Coxeter counting has the following properties.*

(i) *Each $\mathfrak{T}(\mu, \nu)$ is a well-defined non-negative integer.*

(ii) $\mathfrak{T}(\mu, \nu) = 0$ *if and only if* $\mu = \nu$.

(iii) $\mathfrak{T}(\mu, \nu) = 1$ *if and only if μ and ν are consecutive vertices or* $\{\mu, \nu\} \in \mathfrak{T}$.

(iv) $\mathfrak{T}(\mu, \nu) = \mathfrak{T}(\nu, \mu)$.

(v) *If the arcs $\{\mu, \nu\}$ and $\{\pi, \rho\}$ cross, then we have the following Ptolemy relation illustrated by Figure 14.*

$$\mathfrak{T}(\mu, \nu)\mathfrak{T}(\pi, \rho) = \mathfrak{T}(\mu, \pi)\mathfrak{T}(\nu, \rho) + \mathfrak{T}(\mu, \rho)\mathfrak{T}(\nu, \pi).$$

(vi) *If μ^-, μ, μ^+ are three consecutive vertices then*

$$\mathfrak{T}(\mu^-, \mu^+) = 1 + (\textit{the number of arcs in } \mathfrak{T} \textit{ ending at } \mu).$$

Proof. By Remark 2.2, the case of a good triangulation of D_n reduces to the case of a triangulation of a finite polygon. In this case, all the properties are well-known; indeed, (i) through (iii) are clear from Definition 2.1 and Remark 2.2. For (iv) see [7, cor. 1], for (v) see [21, sec. 4.2], and for (vi) see (27) in [9] and [10] or [21, thm. 4.3]. □

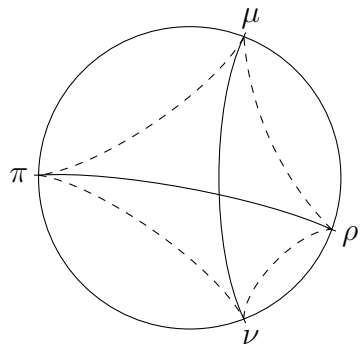

FIGURE 14. The arcs $\{\mu, \nu\}$ and $\{\pi, \rho\}$ cross since $\mu < \pi < \nu < \rho$. The crossing gives the Ptolemy relation $\mathfrak{T}(\mu, \nu)\mathfrak{T}(\pi, \rho) = \mathfrak{T}(\mu, \pi)\mathfrak{T}(\nu, \rho) + \mathfrak{T}(\mu, \rho)\mathfrak{T}(\nu, \pi)$.

3. SL$_2$-tilings in the abstract and SL$_2$-tilings arising from triangulations of the disc

Definition 3.1. Let $A \subseteq \mathbb{Z} \times \mathbb{Z}$ be given. A *partial* SL$_2$*-tiling defined on* A is a map $t : A \to \{1, 2, 3, \ldots\}$ such that

$$\begin{vmatrix} t(i,j) & t(i,j+1) \\ t(i+1,j) & t(i+1,j+1) \end{vmatrix} = 1$$

whenever the determinant makes sense.

The values of t are called *entries* of the partial SL$_2$-tiling. We always write the entries $t(i, j)$ in matrix style, so i increases when we move down, j increases when we move right. Compass directions and words like *row*, *column*, *first quadrant*, and *third quadrant* are to be interpreted in this context, see Figure 15.

If $A = \mathbb{Z} \times \mathbb{Z}$ then t is simply called an SL$_2$*-tiling*, see Figure 3.

If $A = \{(i, j) \mid i < j\}$ and $t(i, i + 1) = 1$ for each i, then t is called an *infinite frieze*, see Figure 5. Infinite friezes were introduced in [24, def. 1.1]. Note that we index them differently from [24] to improve compatibility with SL$_2$-tilings. When t is an infinite frieze, we set $t(i, i) = 0$.

If A is a diagonal band running northwest to southeast and t is equal to 1 on both edges of the band, then t is called a *Conway–Coxeter frieze*. These were introduced in [9] and [10] where the band is typeset horizontally, that is, rotated by 45 degrees anticlockwise compared to our notation, see Figure 1.

By (21) in [9] and [10], a Conway–Coxeter frieze has a fundamental domain which is the restriction $t\,|_F$ of the frieze t to a triangle F as shown in Figure 17. The lower edge of the frieze is the diagonal with all entries equal to 1. The upper edge of the frieze contains the 1 at the upper right corner of the triangle. The entries of the whole frieze are obtained by tiling the diagonal band A with translations of $t\,|_F$ and its reflection in a line running northwest to southeast.

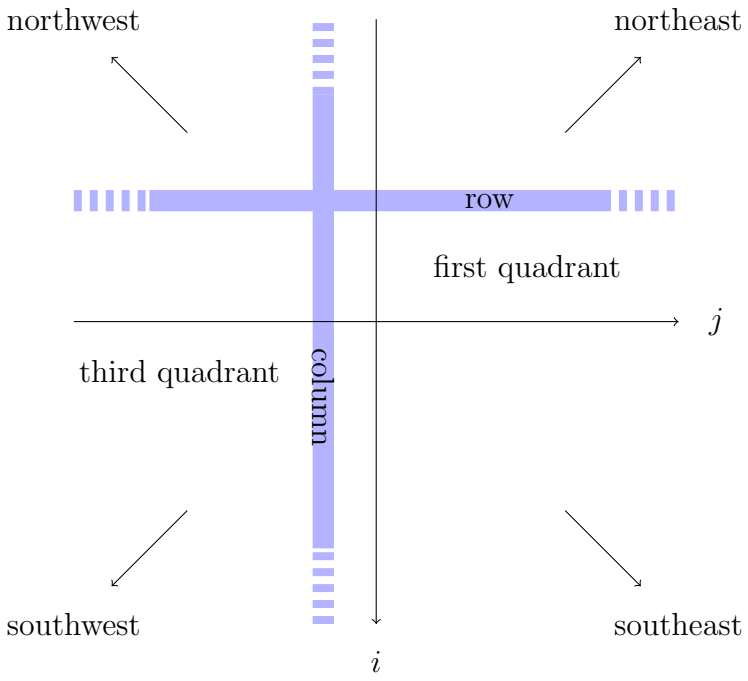

FIGURE 15. When writing the entries $t(i, j)$ of an SL_2-tiling t, we use matrix style so i increases downwards, j increases to the right.

Setup 3.2. Throughout, t is an SL_2-tiling. Recall from [18, sec. 5] that there are associated infinite friezes p and q defined by

$$p(a,d) = \begin{vmatrix} t(a,w) & t(a,w+1) \\ t(d,w) & t(d,w+1) \end{vmatrix} \quad , \quad q(u,x) = \begin{vmatrix} t(c,u) & t(c,x) \\ t(c+1,u) & t(c+1,x) \end{vmatrix}$$

for integers $a \leqslant d$, $u \leqslant x$. Note that the integers w and c can be chosen freely by [18, rmk. 5.2], and that $p(a,d)$ and $q(u,x)$ are indeed positive for $a < d$ and $u < x$ by [18, prop. 5.6].

Lemma 3.3. *We have the following Ptolemy relations.*

(i) Let $a < b < c < d$ be integers. Then

$$p(a,c)p(b,d) = p(a,b)p(c,d) + p(a,d)p(b,c) \quad \text{and} \quad q(a,c)q(b,d) = q(a,b)q(c,d) + q(a,d)q(b,c).$$

(ii) Let v and $a < b < c$ be integers. Then

$$p(a,c)t(b,v) = p(b,c)t(a,v) + p(a,b)t(c,v) \quad \text{and} \quad q(a,c)t(v,b) = q(b,c)t(v,a) + q(a,b)t(v,c).$$

(iii) Let $b < c$ and $v < w$ be integers. Then

$$t(b,v)t(c,w) = t(b,w)t(c,v) + p(b,c)q(v,w).$$

Proof. See [18], propositions 5.4, 5.5, and 5.7. □

Lemma 3.4. *Let i, m be integers with $m > 0$. The entry m occurs only finitely many times in each of the following (half-)rows and (half)-columns:*

$$t(i,-)\ ,\ t(-,i)\ ,\ p(i,-)\ ,\ p(-,i)\ ,\ q(i,-)\ ,\ q(-,i).$$

Proof. The statements about $t(i,-)$ and $t(-,i)$ are [18, prop. 6.1]. The proof of that result can be modified as follows to show the remaining statements:

Suppose that $i < j < k$ are integers with $p(i,j) = p(i,k) = m$. The Ptolemy relation 3.3(i) gives

$$p(i-1,j)p(i,k) = p(i-1,i)p(j,k) + p(i-1,k)p(i,j) = p(j,k) + p(i-1,k)p(i,j)$$

whence

$$p(j,k) = \begin{vmatrix} p(i-1,j) & p(i-1,k) \\ p(i,j) & p(i,k) \end{vmatrix} = \begin{vmatrix} p(i-1,j) & p(i-1,k) \\ m & m \end{vmatrix} = m \cdot \big(p(i-1,j) - p(i-1,k)\big).$$

Since $p(j,k) > 0$ we learn $p(i-1,j) > p(i-1,k)$.

Hence if there is a sequence of integers $i < j < k < \cdots$ with $p(i,j) = p(i,k) = \cdots = m$, then $p(i-1,j) > p(i-1,k) > \cdots$. Since the entries of p are non-negative, this implies that the sequence is finite, so the half-row $p(i,-)$ has only finitely many entries equal to m.

The remaining claims are proved symmetrically. □

Proposition 3.5. *Let $\mathfrak{T}$ be a good triangulation of D_n, the disc with n accumulation points where $n \in \{2,3,4\}$.*

(i) The map $(b,v) \mapsto \mathfrak{T}(b^{\mathrm{I}}, v^{\mathrm{III}})$ is an SL_2-tiling.

(ii) The map $(a,d) \mapsto \mathfrak{T}(a^{\mathrm{I}}, d^{\mathrm{I}})$ is an infinite frieze defined in the half plane $\{(a,d) \mid a \leqslant d\}$.

(iii) The map $(u,x) \mapsto \mathfrak{T}(u^{\mathrm{III}}, x^{\mathrm{III}})$ is an infinite frieze defined in the half plane $\{(u,x) \mid u \leqslant x\}$.

Proof. (i) We have

$$\begin{aligned} &\begin{vmatrix} \mathfrak{T}(b^{\mathrm{I}}, v^{\mathrm{III}}) & \mathfrak{T}\big(b^{\mathrm{I}}, (v+1)^{\mathrm{III}}\big) \\ \mathfrak{T}\big((b+1)^{\mathrm{I}}, v^{\mathrm{III}}\big) & \mathfrak{T}\big((b+1)^{\mathrm{I}}, (v+1)^{\mathrm{III}}\big) \end{vmatrix} \\ &\quad = \mathfrak{T}(b^{\mathrm{I}}, v^{\mathrm{III}})\mathfrak{T}\big((b+1)^{\mathrm{I}}, (v+1)^{\mathrm{III}}\big) - \mathfrak{T}\big(b^{\mathrm{I}}, (v+1)^{\mathrm{III}}\big)\mathfrak{T}\big((b+1)^{\mathrm{I}}, v^{\mathrm{III}}\big) \\ &\quad = \mathfrak{T}\big(b^{\mathrm{I}}, (b+1)^{\mathrm{I}}\big)\mathfrak{T}\big(v^{\mathrm{III}}, (v+1)^{\mathrm{III}}\big) \\ &\quad = 1, \end{aligned}$$

where the second equality is by the Ptolemy relation in Lemma 2.3(v) and the last equality is by Lemma 2.3(iii).

(ii) and (iii) are analogous to (i). □

Remark 3.6. As explained, the point of the paper is to show that *every* SL_2-tiling arises as in Proposition 3.5(i).

Definition 3.7. The SL_2-tiling $(b,v) \mapsto \mathfrak{T}(b^{\mathrm{I}}, v^{\mathrm{III}})$ from Proposition 3.5(i) is said to *arise from $\mathfrak{T}$ by Conway–Coxeter counting*. It will be denoted $\Phi(\mathfrak{T})$.

Lemma 3.8. *Let t be an SL_2-tiling with associated infinite friezes p, q. Let $\mathfrak{T}$ be a good triangulation of D_n.*

On the one hand, assume $t = \Phi(\mathfrak{T})$, that is, $t(b,v) = \mathfrak{T}(b^{\mathrm{I}}, v^{\mathrm{III}})$ for all integers b, v. Then

(i) $p(b-1,b+1) = \mathfrak{T}\big((b-1)^{\mathrm{I}}, (b+1)^{\mathrm{I}}\big)$ for each b,

(ii) $q(v-1,v+1) = \mathfrak{T}\big((v-1)^{\mathrm{III}}, (v+1)^{\mathrm{III}}\big)$ for each v.

On the other hand, assume that (i) and (ii) hold along with at least one of the following two conditions.

(iii) There are integers $e < f$ and $g < h$ such that
$$t(e,g) = \mathfrak{T}(e^{\mathrm{I}}, g^{\mathrm{III}}) \ , \ t(f,g) = \mathfrak{T}(f^{\mathrm{I}}, g^{\mathrm{III}}) \ , \ t(f,h) = \mathfrak{T}(f^{\mathrm{I}}, h^{\mathrm{III}}).$$
(iii)' There are integers $e < f$ and $g < h$ such that
$$t(e,h) = \mathfrak{T}(e^{\mathrm{I}}, h^{\mathrm{III}}) \ , \ t(f,g) = \mathfrak{T}(f^{\mathrm{I}}, g^{\mathrm{III}}) \ , \ t(f,h) = \mathfrak{T}(f^{\mathrm{I}}, h^{\mathrm{III}}).$$

Then $t = \Phi(\mathfrak{T})$, that is, $t(b,v) = \mathfrak{T}(b^{\mathrm{I}}, v^{\mathrm{III}})$ for all b and v.

Proof. "On the one hand": Let b be a given integer and pick an arbitrary integer v. Then
$$\begin{aligned} p(b-1,b+1)t(b,v) &= p(b-1,b)t(b+1,v) + p(b,b+1)t(b-1,v) \\ &= t(b+1,v) + t(b-1,v) \end{aligned}$$
where the first equality is by the Ptolemy relation in Lemma 3.3(ii). Moreover,
$$\begin{aligned} &\mathfrak{T}\big((b-1)^{\mathrm{I}}, (b+1)^{\mathrm{I}}\big)\mathfrak{T}(b^{\mathrm{I}}, v^{\mathrm{III}}) \\ &\quad = \mathfrak{T}\big((b-1)^{\mathrm{I}}, b^{\mathrm{I}}\big)\mathfrak{T}\big((b+1)^{\mathrm{I}}, v^{\mathrm{III}}\big) + \mathfrak{T}\big(b^{\mathrm{I}}, (b+1)^{\mathrm{I}}\big)\mathfrak{T}\big((b-1)^{\mathrm{I}}, v^{\mathrm{III}}\big) \\ &\quad = \mathfrak{T}\big((b+1)^{\mathrm{I}}, v^{\mathrm{III}}\big) + \mathfrak{T}\big((b-1)^{\mathrm{I}}, v^{\mathrm{III}}\big) \end{aligned}$$
where the first equality is by the Ptolemy relation in Lemma 2.3(v) and the second equality is by Lemma 2.3(iii).

By assumption, we have $t(c,v) = \mathfrak{T}(c^{\mathrm{I}}, v^{\mathrm{III}})$ for each c. In particular this holds for c equal to $b-1$, b, or $b+1$. The two displayed equations therefore combine to give $p(b-1,b+1) = \mathfrak{T}\big((b-1)^{\mathrm{I}}, (b+1)^{\mathrm{I}}\big)$. This shows (i), and (ii) follows by symmetry.

"On the other hand": Consider the infinite friezes p and $(a,d) \mapsto \mathfrak{T}(a^{\mathrm{I}}, d^{\mathrm{I}})$, see Proposition 3.5(ii). Condition (i) says that they agree on the diagonal $\{(b-1,b+1) \mid b \in \mathbb{Z}\}$. However, it is easy to see that an infinite frieze is determined entirely by its values on this diagonal which is also known as its quiddity sequence; see [24, rmk. 1.3]. So the two infinite friezes agree:
$$p(a,d) = \mathfrak{T}(a^{\mathrm{I}}, d^{\mathrm{I}}) \text{ for } a \leqslant d. \tag{3.1}$$
Similarly, condition (ii) implies
$$q(u,x) = \mathfrak{T}(u^{\mathrm{III}}, x^{\mathrm{III}}) \text{ for } u \leqslant x. \tag{3.2}$$

Now suppose condition (iii) holds. If $b < e$ then the Ptolemy relation in 3.3(ii) says
$$p(b,f)t(e,g) = p(b,e)t(f,g) + p(e,f)t(b,g) \tag{3.3}$$
while the Ptolemy relation in Lemma 2.3(v) says
$$\mathfrak{T}(b^{\mathrm{I}}, f^{\mathrm{I}})\mathfrak{T}(e^{\mathrm{I}}, g^{\mathrm{III}}) = \mathfrak{T}(b^{\mathrm{I}}, e^{\mathrm{I}})\mathfrak{T}(f^{\mathrm{I}}, g^{\mathrm{III}}) + \mathfrak{T}(e^{\mathrm{I}}, f^{\mathrm{I}})\mathfrak{T}(b^{\mathrm{I}}, g^{\mathrm{III}}). \tag{3.4}$$
Equations (3.1) and (3.2) and condition (iii) say that the first five of the six factors in Equation (3.3) are equal to the corresponding factors in Equation (3.4). Hence the last factors are also equal, so
$$t(b,g) = \mathfrak{T}(b^{\mathrm{I}}, g^{\mathrm{III}}) \text{ for } b < e.$$

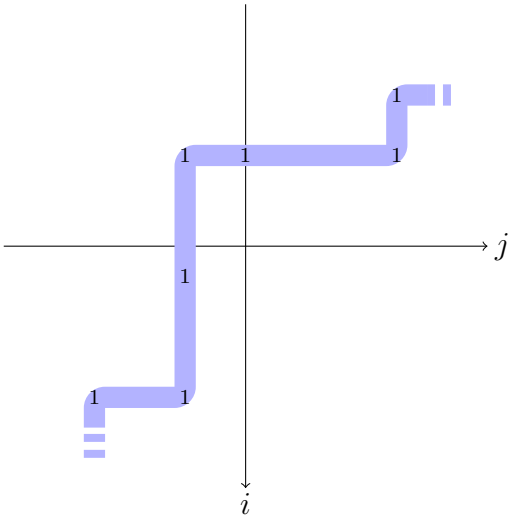

FIGURE 16. The entries of t which are equal to 1 occur on a zig-zag which can be bounded or unbounded to each side.

Similar arguments can be applied for $e < b < f$ and $f < b$, and the cases $b = e$ and $b = f$ are handled by condition (iii) itself, so we get

$$t(b, g) = \mathfrak{T}(b^{\mathrm{I}}, g^{\mathrm{III}}) \text{ for each } b.$$

Similar arguments prove that

$$t(f, v) = \mathfrak{T}(f^{\mathrm{I}}, v^{\mathrm{III}}) \text{ for each } v.$$

Hence the SL_2-tilings t and $(b, v) \mapsto \mathfrak{T}(b^{\mathrm{I}}, v^{\mathrm{III}})$ match on column number g and row number f. However, it is easy to see that an SL_2-tiling is determined entirely by its values on a column and a row, so the two SL_2-tilings must agree everywhere as claimed.

If condition (iii)' holds then we proceed symmetrically. □

Lemma 3.9. *If t has entries which are equal to 1, then they occur on a zig-zag as shown in Figure 16. The zig-zag is bounded or unbounded to each side.*

More formally, there is an interval $K \subseteq \mathbb{Z}$ which is bounded or unbounded to each side, along with coordinate pairs (b_k, v_k) for $k \in K$ such that the following hold.

- *(i) $t(b, v) = 1$ if and only if $(b, v) = (b_k, v_k)$ for some $k \in K$.*
- *(ii) For each $k \neq \max(K)$, we have precisely one of the following two options:*
  - *(a) $b_{k+1} < b_k$ and $v_{k+1} = v_k$ or*
  - *(b) $b_{k+1} = b_k$ and $v_{k+1} > v_k$.*
- *(iii) If K is unbounded above, then there are infinitely many shifts between options (a) and (b) when k increases.*
- *(iv) If K is unbounded below, then there are infinitely many shifts between options (a) and (b) when k decreases.*

Proof. The proof of [18, prop. 8.2] works. □

Remark 3.10. Lemma 3.9 says that the zig-zag of 1's in t, shown in Figure 16, is bounded or unbounded to each side. There are hence four possibilities which can all be realised, as one can see in the SL_2-tilings $t = \Phi(\mathfrak{T})$ for various choices of the triangulation $\mathfrak{T}$.

Namely, by Lemma 2.3(iii), the 1's in t correspond to the arcs in $\mathfrak{T}$ which connect intervals I and III.

It follows that if $\mathfrak{T}$ has the form in Figure 20, then the zig-zag of 1's in t is unbounded to both sides. That is, t has infinitely many 1's in both the first and the third quadrant.

If $\mathfrak{T}$ has the form in Figure 21, then the zig-zag is bounded to the left and unbounded to the right. That is, t has infinitely many 1's in the first, but not the third quadrant. The opposite situation can be obtained by reflecting $\mathfrak{T}$ in a vertical line.

If $\mathfrak{T}$ has the form in Figure 22, then the zig-zag is bounded to the left and to the right. That is, t has only finitely many 1's.

Finally, note that if $\mathfrak{T}$ has the form in Figure 29, then t has no entries equal to 1. This corresponds to $K = \emptyset$ in Lemma 3.9.

4. The partial triangulation $\Theta(t)$ of an SL_2-tiling t

Recall that t is a fixed SL_2-tiling with associated infinite friezes p and q, see Setup 3.2.

Definition 4.1 (The partial triangulation $\Theta(t)$)**.** We define a set of arcs in D_n as follows.

$$\Theta(t) = \big\{\{b^{\mathrm{I}}, v^{\mathrm{III}}\} \,\big|\, t(b,v) = 1\big\} \cup \big\{\{a^{\mathrm{I}}, d^{\mathrm{I}}\} \,\big|\, a+2 \leqslant d,\, p(a,d) = 1\big\} \cup \big\{\{u^{\mathrm{III}}, x^{\mathrm{III}}\} \,\big|\, u+2 \leqslant x,\, q(u,x) = 1\big\}.$$

The definition makes sense since intervals I and III are always present on the boundary of D_n; see Definitions 1.3 and 1.4.

Remark 4.2. We remind the reader that when t is given and we seek to construct a good triangulation $\mathfrak{T}$ of D_n such that $t = \Phi(\mathfrak{T})$, we will do so by adding arcs to $\Theta(t)$.

Lemma 4.3. *The set $\Theta(t)$ is a partial triangulation of D_n.*

Proof. If the internal arcs $\{a^{\mathrm{I}}, c^{\mathrm{I}}\}$ and $\{b^{\mathrm{I}}, d^{\mathrm{I}}\}$ cross, then we can suppose $a < b < c < d$. Then the Ptolemy relation in Lemma 3.3(i) says

$$p(a,c)p(b,d) = p(a,b)p(c,d) + p(a,d)p(b,c) \geqslant 2,$$

where the inequality holds since each of $p(a,b)$, $p(c,d)$, $p(a,d)$, $p(b,c)$ is a positive integer. Hence $p(a,c)$ and $p(b,d)$ cannot both be equal to 1, so $\{a^{\mathrm{I}}, c^{\mathrm{I}}\}$ and $\{b^{\mathrm{I}}, d^{\mathrm{I}}\}$ cannot both be in $\Theta(t)$.

A crossing of an internal arc and a connecting arc is handled similarly by means of Lemma 3.3(ii), and a crossing of two connecting arcs is handled by means of Lemma 3.3(iii). □

Lemma 4.4. *The partial triangulation $\Theta(t)$ is locally finite in the sense of Definition 1.9.*

Proof. Consider the arcs in $\Theta(t)$ which end at the vertex $\mu = b^{\mathrm{I}}$ in interval I. By Definition 4.1 they correspond to the entries which are equal to 1 in the row $t(b,-)$ and the half-rows $p(b,-)$ and $p(-,b)$. By Lemma 3.4 there are only finitely many such entries.

The arcs in $\Theta(t)$ which end at the vertex $\mu = v^{\mathrm{III}}$ in interval III are handled by symmetry. □

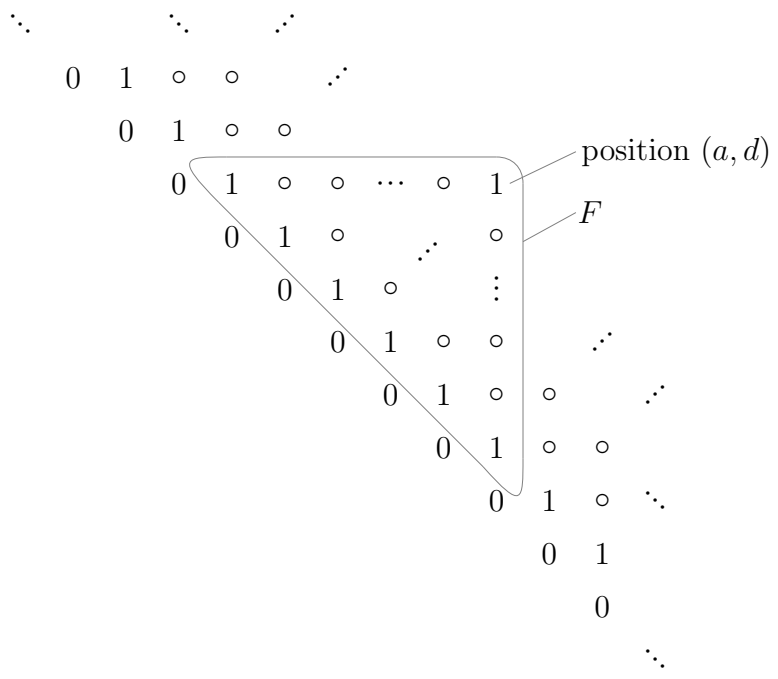

FIGURE 17. Assume that $d \geqslant a+2$ and that the entry at position (a,d) in the infinite frieze p is equal to 1. Then the restriction of p to the triangle F is the fundamental domain of a Conway–Coxeter frieze.

Lemma 4.5. *Let $a < d$ be such that $\{a^{\mathrm{I}}, d^{\mathrm{I}}\} \in \Theta(t)$ or $\{a^{\mathrm{I}}, d^{\mathrm{I}}\}$ is an edge, and let P denote the finite polygon below $\{a^{\mathrm{I}}, d^{\mathrm{I}}\}$, see Definition 1.10 and the left half of Figure 12.*

(i) The restriction $\Theta(t)_P$ is a triangulation of P.

(ii) Conway-Coxeter counting on $\Theta(t)_P$ agrees with a certain part of the infinite frieze p in the following sense: If $a \leqslant b \leqslant c \leqslant d$, then

$$p(b,c) = \Theta(t)_P(b^{\mathrm{I}}, c^{\mathrm{I}}).$$

Proof. If $\{a^{\mathrm{I}}, d^{\mathrm{I}}\}$ is an edge then P is a 2-gon and the lemma is trivial, so suppose $\{a^{\mathrm{I}}, d^{\mathrm{I}}\} \in \Theta(t)$. In particular $\{a^{\mathrm{I}}, d^{\mathrm{I}}\}$ is an arc so $d \geqslant a+2$.

The infinite frieze p is defined on the half plane $\{(b,c) \in \mathbb{Z} \times \mathbb{Z} \mid b < c\}$ and we have $p(b, b+1) = 1$ for each b. Recall that we set $p(b,b) = 0$ so p is as shown in Figure 17. The condition $\{a^{\mathrm{I}}, d^{\mathrm{I}}\} \in \Theta(t)$ means $p(a,d) = 1$. In the figure, this entry is at the upper right corner of the triangle

$$F = \{(b,c) \mid a \leqslant b < c \leqslant d\},$$

and it implies that the restriction $p|_F$ coincides with the fundamental domain of a Conway–Coxeter frieze s. This follows from (10) in [9] and [10]; see also [18, lem. 7.1].

The elements (b,c) of F correspond to the edges and arcs $\{b^{\mathrm{I}}, c^{\mathrm{I}}\}$ of the polygon with vertices $a^{\mathrm{I}}, \ldots, d^{\mathrm{I}}$, that is, the polygon P. Hence the frieze s corresponds to a triangulation $\mathfrak{S}$ of P; specifically,

$$\mathfrak{S} = \big\{\{b^{\mathrm{I}}, c^{\mathrm{I}}\} \text{ is an arc of } P \,\big|\, s(b,c) = 1\big\}.$$

This is due to [9], [10], and more details are given in [7, sec. 2]. Since s and p agree on F, the equation shows that $\mathfrak{S}$ consists of some of the arcs in $\Theta(t)$. Indeed, $\mathfrak{S}$ is precisely the restriction $\Theta(t)_P$ of $\Theta(t)$ to P. Hence $\Theta(t)_P$ is a triangulation of P, proving part (i) of the lemma.

The same references show that, conversely, the fundamental region of the frieze s can be obtained by Conway–Coxeter counting on $\mathfrak{S}$, namely if $\{b^{\mathrm{I}}, c^{\mathrm{I}}\}$ is an edge or an arc of P then

$$s(b,c) = \mathfrak{S}(b^{\mathrm{I}}, c^{\mathrm{I}}).$$

This gives part (ii) of the lemma for $b < c$ because s and p agree on F while $\mathfrak{S} = \Theta(t)_P$. If $b = c$ then part (ii) of the lemma is trivially true. □

Lemma 4.6. *Let $u < x$ be such that $\{u^{\mathrm{III}}, x^{\mathrm{III}}\} \in \Theta(t)$ or $\{u^{\mathrm{III}}, x^{\mathrm{III}}\}$ is an edge, and let Q denote the finite polygon below $\{u^{\mathrm{III}}, x^{\mathrm{III}}\}$.*

(i) The restriction $\Theta(t)_Q$ is a triangulation of Q.

(ii) Conway-Coxeter counting on $\Theta(t)_Q$ agrees with a certain part of the infinite frieze q in the following sense: If $u \leqslant v \leqslant w \leqslant x$, then

$$q(v,w) = \Theta(t)_Q(v^{\mathrm{III}}, w^{\mathrm{III}}).$$

Proof. Follows from Lemma 4.5 by symmetry. □

Lemma 4.7. *Let $a \leqslant d$ and $u \leqslant x$ be such that $\{a^{\mathrm{I}}, x^{\mathrm{III}}\}, \{d^{\mathrm{I}}, u^{\mathrm{III}}\} \in \Theta(t)$ and let R denote the finite polygon between the arcs $\{a^{\mathrm{I}}, x^{\mathrm{III}}\}$ and $\{d^{\mathrm{I}}, u^{\mathrm{III}}\}$, see the right half of Figure 12.*

(i) The restriction $\Theta(t)_R$ is a triangulation of R.

(ii) Conway-Coxeter counting on $\Theta(t)_R$ agrees with certain parts of the SL_2-tiling t and the infinite friezes p, q in the following sense: If $a \leqslant b \leqslant c \leqslant d$ and $u \leqslant v \leqslant w \leqslant x$, then

$$t(b,v) = \Theta(t)_R(b^{\mathrm{I}}, v^{\mathrm{III}}) \ , \ p(b,c) = \Theta(t)_R(b^{\mathrm{I}}, c^{\mathrm{I}}) \ , \ q(v,w) = \Theta(t)_R(v^{\mathrm{III}}, w^{\mathrm{III}}).$$

Proof. If $\{a^{\mathrm{I}}, x^{\mathrm{III}}\} = \{d^{\mathrm{I}}, u^{\mathrm{III}}\}$ then R is a 2-gon and the lemma is trivial, so suppose that $\{a^{\mathrm{I}}, x^{\mathrm{III}}\}$ and $\{d^{\mathrm{I}}, u^{\mathrm{III}}\}$ are distinct.

Then the proof is analogous to that of Lemma 4.5, except that a more sophisticated method is needed to obtain a fundamental region of a Conway–Coxeter frieze. Specifically, $\{a^{\mathrm{I}}, x^{\mathrm{III}}\}$, $\{d^{\mathrm{I}}, u^{\mathrm{III}}\} \in \Theta(t)$ implies $t(a,x) = t(d,u) = 1$, and these two entries of t span a rectangle in the plane to which t can be restricted. It is shown in [18, prop. 7.2 and fig. 15] how to position suitable restrictions of p and q next to the rectangle in order to obtain a partial SL_2-tiling defined on a triangle F. As in the proof of Lemma 4.5, this tiling coincides with the fundamental region of a Conway–Coxeter frieze, and the proof then proceeds as for Lemma 4.5. □

5. Saturated vertices and defects associated to an SL_2-tiling

Recall that t is a fixed SL_2-tiling with associated infinite friezes p and q, see Setup 3.2.

Definition 5.1 (Vertices strictly below and strictly between arcs)**.** Let $\mathrm{J}, \mathrm{K} \in \{\mathrm{I}, \mathrm{II}, \mathrm{III}, \mathrm{IV}\}$ be intervals of the boundary of D_n.

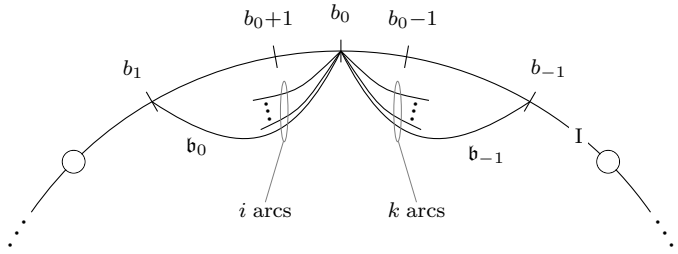

FIGURE 18. This sketch shows $\Theta(t)$ when it has no connecting arcs ending at b_0^{I}. There are i internal arcs in $\Theta(t)$ which go anticlockwise from b_0^{I} and the longest is $\mathfrak{b}_0 = \{b_0^{\mathrm{I}}, b_1^{\mathrm{I}}\}$. There are k internal arcs in $\Theta(t)$ which go clockwise from b_0^{I} and the longest is $\mathfrak{b}_{-1} = \{b_0^{\mathrm{I}}, b_{-1}^{\mathrm{I}}\}$.

(i) If $a \leqslant d-2$ then the vertices $(a+1)^{\mathrm{J}}$, …, $(d-1)^{\mathrm{J}}$ are said to be *strictly below the (internal) arc* $\{a^{\mathrm{J}}, d^{\mathrm{J}}\}$, see the left half of Figure 12.

(ii) If $a \leqslant d$ and $u \leqslant x$ are such that $\{a^{\mathrm{J}}, x^{\mathrm{K}}\}, \{d^{\mathrm{J}}, u^{\mathrm{K}}\}$ are distinct arcs, then the vertices $(a+1)^{\mathrm{J}}$, …, $(d-1)^{\mathrm{J}}, (u+1)^{\mathrm{K}}$, …, $(x-1)^{\mathrm{K}}$ are said to be *strictly between the (connecting) arcs* $\{a^{\mathrm{J}}, x^{\mathrm{K}}\}, \{d^{\mathrm{J}}, u^{\mathrm{K}}\}$, see the right half of Figure 12.

Definition 5.2 (Saturated vertices)**.** A vertex of intervals I or III is called *saturated* if it is strictly below an internal arc $\{a^{\mathrm{I}}, d^{\mathrm{I}}\}$ or $\{u^{\mathrm{III}}, x^{\mathrm{III}}\}$ in $\Theta(t)$, or strictly between two connecting arcs $\{a^{\mathrm{I}}, x^{\mathrm{III}}\}, \{d^{\mathrm{I}}, u^{\mathrm{III}}\}$ in $\Theta(t)$; see Definition 5.1.

A vertex of intervals I or III which is not saturated is called *non-saturated*.

Remark 5.3. Suppose $\{a^{\mathrm{I}}, d^{\mathrm{I}}\} \in \Theta(t)$ and let P denote the finite polygon below the internal arc $\{a^{\mathrm{I}}, d^{\mathrm{I}}\}$. If $a < b < d$ then

$$p(b-1, b+1) = 1 + (\text{the number of arcs in } \Theta(t) \text{ ending at } b^{\mathrm{I}}).$$

This follows from Lemmas 4.5 and 2.3(vi). A similar equality holds for q. In general, there is no such equality, and this is captured by the *defects* introduced in the next definition.

In due course, the defects will be used to augment the partial triangulation $\Theta(t)$ to a triangulation $\mathfrak{T}$ which satisfies

$$p(a, d) = \mathfrak{T}(a^{\mathrm{I}}, d^{\mathrm{I}})$$

for all $a \leqslant d$. In turn, this will permit us to use Lemma 3.8 to prove

$$t(b, v) = \mathfrak{T}(b^{\mathrm{I}}, v^{\mathrm{III}})$$

for all b, v, that is, to prove $t = \Phi(\mathfrak{T})$.

Definition 5.4. The *p-defect* of an integer b is

$$\mathrm{def}_p(b) = p(b-1, b+1) - 1 - (\text{the number of arcs in } \Theta(t) \text{ ending at } b^{\mathrm{I}})$$

and the *q-defect* of an integer v is

$$\mathrm{def}_q(v) = q(v-1, v+1) - 1 - (\text{the number of arcs in } \Theta(t) \text{ ending at } v^{\mathrm{III}}).$$

Lemma 5.5. *Suppose that $\Theta(t)$ has no connecting arcs which end at the vertex b_0^{I}. We use the following notation, illustrated by Figure 18, which makes sense because $\Theta(t)$ is locally finite by Lemma 4.4:*

Let $\mathfrak{b}_0 = \{b_0^{\mathrm{I}}, b_1^{\mathrm{I}}\}$ be either the longest internal arc in $\Theta(t)$ going anticlockwise from b_0^{I}, or, if there are no such arcs, the edge going anticlockwise from b_0^{I}.

Let $\mathfrak{b}_{-1} = \{b_{-1}^{\mathrm{I}}, b_0^{\mathrm{I}}\}$ be either the longest internal arc in $\Theta(t)$ going clockwise from b_0^{I}, or, if there are no such arcs, the edge going clockwise from b_0^{I}.

Then

$$\mathrm{def}_p(b_0) = p(b_{-1}, b_1) - 1.$$

Proof. The special cases where $\mathfrak{b}_0$ or $\mathfrak{b}_{-1}$ is an edge are omitted since they are easy. We assume that $\mathfrak{b}_0$ and $\mathfrak{b}_{-1}$ are arcs.

We let i, respectively k, denote the number of internal arcs in $\Theta(t)$ going anticlockwise, respectively clockwise, from b_0^{I}, see Figure 18.

First, consider the finite polygon P below $\mathfrak{b}_0$. Lemma 4.5 says that $\Theta(t)$ restricts to a triangulation $\Theta(t)_P$ of P and that

$$p(b_0 + 1, b_1) = \Theta(t)_P\big((b_0 + 1)^{\mathrm{I}}, b_1^{\mathrm{I}}\big) = (*).$$

Viewed in P, the vertices $(b_0 + 1)^{\mathrm{I}}$, b_0^{I}, b_1^{I} are consecutive so Lemma 2.3(vi) gives

$$(*) = 1 + (\text{the number of arcs in } \Theta(t)_P \text{ ending at } b_0^{\mathrm{I}}) = (**).$$

The arcs in $\Theta(t)_P$ ending at b_0^{I} are precisely the arcs in $\Theta(t)$ going anticlockwise from b_0^{I}, except for $\mathfrak{b}_0$ which is an edge of P. Hence

$$(**) = i.$$

This proves the first of the following equalities, and the second follows by symmetry.

$$p(b_0 + 1, b_1) = i, \tag{5.1}$$

$$p(b_{-1}, b_0 - 1) = k. \tag{5.2}$$

Secondly, we show two consequences of the Ptolemy relations in Lemma 3.3.

- Since $\mathfrak{b}_0 = \{b_0^{\mathrm{I}}, b_1^{\mathrm{I}}\}$ is in $\Theta(t)$, we have

  $$p(b_0, b_1) = 1. \tag{5.3}$$

  This gives the first equality in the following computation,

  $$\begin{aligned} p(b_0 - 1, b_0 + 1) &= p(b_0 - 1, b_0 + 1)p(b_0, b_1) \\ &= p(b_0 - 1, b_0)p(b_0 + 1, b_1) + p(b_0 - 1, b_1)p(b_0, b_0 + 1) \\ &= i + p(b_0 - 1, b_1), \end{aligned} \tag{5.4}$$

  where the second equality is by the Ptolemy relation in Lemma 3.3(i) and the third equality uses Equation (5.1).
- Since $\mathfrak{b}_{-1} = \{b_{-1}^{\mathrm{I}}, b_0^{\mathrm{I}}\}$ is in $\Theta(t)$, we have $p(b_{-1}, b_0) = 1$. This gives the first equality in the following computation,

  $$\begin{aligned} p(b_0 - 1, b_1) &= p(b_{-1}, b_0)p(b_0 - 1, b_1) \\ &= p(b_{-1}, b_0 - 1)p(b_0, b_1) + p(b_{-1}, b_1)p(b_0 - 1, b_0) \\ &= k + p(b_{-1}, b_1), \end{aligned} \tag{5.5}$$

  where the second equality is by the Ptolemy relation in Lemma 3.3(i) and the third equality uses Equations (5.2) and (5.3).

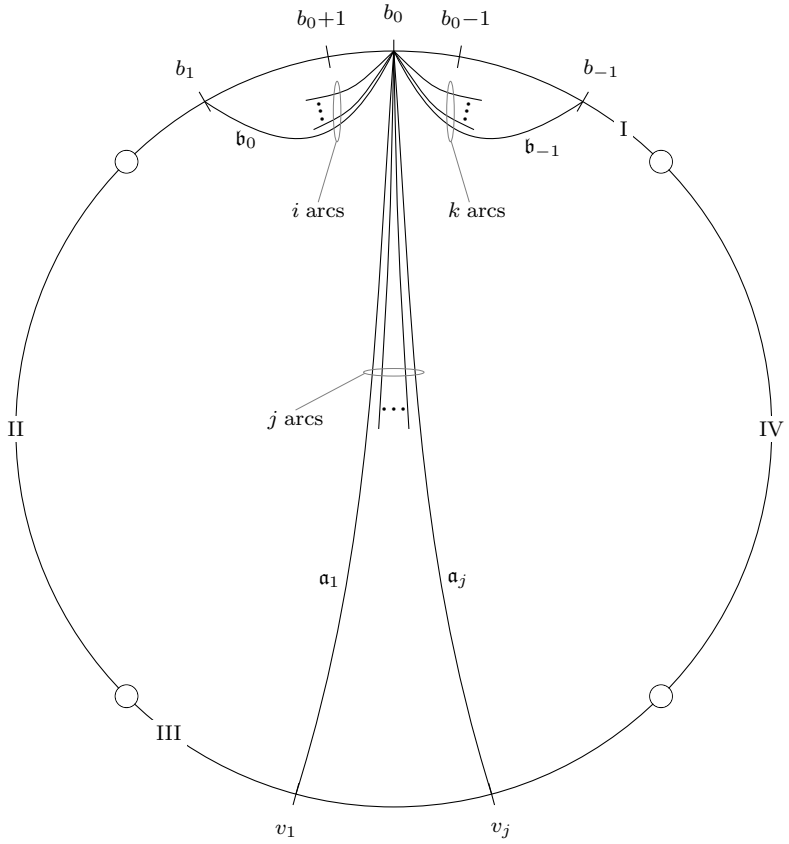

FIGURE 19. This sketch shows $\Theta(t)$ when it contains $j \geqslant 1$ connecting arcs $\mathfrak{a}_1, \ldots, \mathfrak{a}_j$ ending at b_0^{I}. There are i internal arcs in $\Theta(t)$ which go anticlockwise from b_0^{I} and the longest is $\mathfrak{b}_0 = \{b_0^{\mathrm{I}}, b_1^{\mathrm{I}}\}$. There are k internal arcs in $\Theta(t)$ which go clockwise from b_0^{I} and the longest is $\mathfrak{b}_{-1} = \{b_0^{\mathrm{I}}, b_{-1}^{\mathrm{I}}\}$.

Finally, the previous equations combine as follows.

$$p(b_0 - 1, b_0 + 1) \overset{(5.4)}{=} i + p(b_0 - 1, b_1) \overset{(5.5)}{=} i + k + p(b_{-1}, b_1)$$

Subtracting $i + k + 1$ from this equation turns the left hand side into $\mathrm{def}_p(b_0)$ because there are a total of $i+k$ arcs in $\Theta(t)$ which end at b_0^{I}; see Figure 18 and Definition 5.4. This proves the lemma. □

Lemma 5.6. *Suppose that $\Theta(t)$ has at least one connecting arc which ends at the vertex b_0^{I}. We use the following notation, illustrated by Figure 19, which makes sense because $\Theta(t)$ is locally finite by Lemma 4.4:*

Let $v_1 < \cdots < v_j$ be such that $\mathfrak{a}_1 = \{b_0^{\mathrm{I}}, v_1^{\mathrm{III}}\}, \ldots, \mathfrak{a}_j = \{b_0^{\mathrm{I}}, v_j^{\mathrm{III}}\}$ are all the connecting arcs in $\Theta(t)$ which end at b_0^{I}.

Let $\mathfrak{b}_0 = \{b_0^{\mathrm{I}}, b_1^{\mathrm{I}}\}$ be either the longest internal arc in $\Theta(t)$ going anticlockwise from b_0^{I}, or, if there are no such arcs, the edge going anticlockwise from b_0^{I}.

Let $\mathfrak{b}_{-1} = \{b_{-1}^{\mathrm{I}}, b_0^{\mathrm{I}}\}$ be either the longest internal arc in $\Theta(t)$ going clockwise from b_0^{I}, or, if there are no such arcs, the edge going clockwise from b_0^{I}.

Then

$$\mathrm{def}_p(b_0) = t(b_{-1}, v_j) + t(b_1, v_1) - 2.$$

Proof. The special cases where $\mathfrak{b}_0$ or $\mathfrak{b}_{-1}$ is an edge or where $j = 1$ are omitted since they are easy. We assume that $\mathfrak{b}_0$ and $\mathfrak{b}_{-1}$ are arcs and that $j \geqslant 2$.

We let i, respectively k, denote the number of internal arcs in $\Theta(t)$ going anticlockwise, respectively clockwise, from b_0^{I}. The choice of $v_1 < \cdots < v_j$ means that there are j connecting arcs in $\Theta(t)$ ending at b_0^{I}. See Figure 19.

First, an argument like the one used to prove Equation (5.1) shows

$$q(v_1, v_j) = j - 1. \tag{5.6}$$

Secondly, the same arguments as in the proof of Lemma 5.5 show that Equations (5.2), (5.3), and (5.4) remain valid. We collect three other consequences of the Ptolemy relations from Lemma 3.3.

- Since $\mathfrak{a}_1 = \{b_0^{\mathrm{I}}, v_1^{\mathrm{III}}\}$ is in $\Theta(t)$, we have $t(b_0, v_1) = 1$. This gives the first equality in the following computation,

$$\begin{aligned} p(b_0 - 1, b_1) &= p(b_0 - 1, b_1)t(b_0, v_1) \\ &= p(b_0 - 1, b_0)t(b_1, v_1) + p(b_0, b_1)t(b_0 - 1, v_1) \\ &= t(b_1, v_1) + t(b_0 - 1, v_1), \end{aligned} \tag{5.7}$$

  where the second equality is by the Ptolemy relation in Lemma 3.3(ii) and the third equality uses Equation (5.3).

- Since $\mathfrak{a}_j = \{b_0^{\mathrm{I}}, v_j^{\mathrm{III}}\}$ is in $\Theta(t)$, we have $t(b_0, v_j) = 1$. This gives the first equality in the following computation,

$$\begin{aligned} t(b_0 - 1, v_1) &= t(b_0 - 1, v_1)t(b_0, v_j) \\ &= t(b_0 - 1, v_j)t(b_0, v_1) + p(b_0 - 1, b_0)q(v_1, v_j) \\ &= t(b_0 - 1, v_j) + j - 1, \end{aligned} \tag{5.8}$$

  where the second equality is by the Ptolemy relation in Lemma 3.3(iii) and the third equality uses $t(b_0, v_1) = 1$ and Equation (5.6).

- Since $\mathfrak{b}_{-1} = \{b_{-1}^{\mathrm{I}}, b_0^{\mathrm{I}}\}$ is in $\Theta(t)$, we have $p(b_{-1}, b_0) = 1$. This gives the first equality in the following computation,

$$\begin{aligned} t(b_0 - 1, v_j) &= p(b_{-1}, b_0)t(b_0 - 1, v_j) \\ &= p(b_0 - 1, b_0)t(b_{-1}, v_j) + p(b_{-1}, b_0 - 1)t(b_0, v_j) \\ &= t(b_{-1}, v_j) + k, \end{aligned} \tag{5.9}$$

  where the second equality is by the Ptolemy relation in Lemma 3.3(ii) and the third equality uses $t(b_0, v_j) = 1$ and Equation (5.2).

Finally, the previous equations combine as follows.

$$\begin{aligned} p(b_0-1,b_0+1) &\overset{(5.4)}{=} i + p(b_0-1,b_1) \\ &\overset{(5.7)}{=} i + t(b_1,v_1) + t(b_0-1,v_1) \\ &\overset{(5.8)}{=} i + t(b_1,v_1) + t(b_0-1,v_j) + j - 1 \\ &\overset{(5.9)}{=} i + t(b_1,v_1) + t(b_{-1},v_j) + k + j - 1 \end{aligned}$$

Subtracting $i+j+k+1$ from this equation turns the left hand side into $\mathrm{def}_p(b_0)$ because there are a total of $i+j+k$ arcs in $\Theta(t)$ which end at b_0^{I}; see Figure 19 and Definition 5.4. This proves the lemma. □

Lemma 5.7. *(i) b^{I} is saturated if and only if $\mathrm{def}_p(b) = 0$.*

(ii) b^{I} is non-saturated if and only if $\mathrm{def}_p(b) > 0$.

(iii) v^{III} is saturated if and only if $\mathrm{def}_q(v) = 0$.

(iv) v^{III} is non-saturated if and only if $\mathrm{def}_q(v) > 0$.

Proof. To prove parts (i) and (ii), it is enough to prove "only if" in each part.

Part (i), "only if": Let b^{I} be a saturated vertex, see Definition 5.2. There are two cases.

The first case is that b^{I} is strictly below the internal arc $\{a^{\mathrm{I}}, d^{\mathrm{I}}\} \in \Theta(t)$, whence $a < b < d$. Let P denote the finite polygon below $\{a^{\mathrm{I}}, d^{\mathrm{I}}\}$. Lemma 4.5 says that the restriction $\Theta(t)_P$ is a triangulation of P and that

$$p(b-1,b+1) = \Theta(t)_P\big((b-1)^{\mathrm{I}}, (b+1)^{\mathrm{I}}\big) = (*).$$

Lemma 2.3(vi) gives

$$(*) = 1 + (\text{the number of arcs in } \Theta(t)_P \text{ ending at } b^{\mathrm{I}}) = (**).$$

However, $\Theta(t)$ is a partial triangulation of D_n so none of its arcs can cross $\{a^{\mathrm{I}}, d^{\mathrm{I}}\}$. It follows that

$$(**) = 1 + (\text{the number of arcs in } \Theta(t) \text{ ending at } b^{\mathrm{I}}).$$

This shows $\mathrm{def}_p(b) = 0$.

The second case is that b^{I} is strictly between the connecting arcs $\{a^{\mathrm{I}}, x^{\mathrm{III}}\}, \{d^{\mathrm{I}}, u^{\mathrm{III}}\} \in \Theta(t)$. This is handled similarly, replacing Lemma 4.5 by Lemma 4.7.

Part (ii), "only if": Let b^{I} be a non-saturated vertex. There are two cases.

The first case is that there are no connecting arcs in $\Theta(t)$ which end at b^{I}. Set $b_0 = b$ and apply Lemma 5.5; in the notation of the lemma, $\Theta(t)$ at b_0^{I} looks like Figure 18. The lemma gives

$$\mathrm{def}_p(b) = \mathrm{def}_p(b_0) = p(b_{-1},b_1) - 1 = (\dagger).$$

However, since b^{I} is non-saturated, the arc $\{b_{-1}^{\mathrm{I}}, b_1^{\mathrm{I}}\}$ cannot be in $\Theta(t)$. It follows that $p(b_{-1},b_1) > 1$ so $(\dagger) > 0$ as desired.

The second case is that there are connecting arcs in $\Theta(t)$ which end at b^{I}. Set $b_0 = b$ and apply Lemma 5.6; in the notation of the lemma, $\Theta(t)$ at b_0^{I} looks like Figure 19. The lemma gives

$$\mathrm{def}_p(b) = \mathrm{def}_p(b_0) = t(b_{-1},v_j) + t(b_1,v_1) - 2 = (\ddagger).$$

However, since b^{I} is non-saturated, it cannot be that both arcs $\{b^{\mathrm{I}}_{-1}, v^{\mathrm{III}}_j\}$ and $\{b^{\mathrm{I}}_1, v^{\mathrm{III}}_1\}$ are in $\Theta(t)$. It follows that $t(b_{-1}, v_j) > 1$ or $t(b_1, v_1) > 1$ so $(\ddagger) > 0$ as desired.

(iii) and (iv) follow by symmetry. □

Lemma 5.8. *Let $\mathfrak{T}$ be a good triangulation of D_n such that $\Theta(t) \subseteq \mathfrak{T}$.*

(i) b^{I} is saturated $\Rightarrow \mathfrak{T}\big((b-1)^{\mathrm{I}}, (b+1)^{\mathrm{I}}\big) = p(b-1, b+1)$.

(ii) v^{III} is saturated $\Rightarrow \mathfrak{T}\big((v-1)^{\mathrm{III}}, (v+1)^{\mathrm{III}}\big) = q(b-1, b+1)$.

Proof. (i) Since b^{I} is saturated, Lemma 5.7(i) says $\mathrm{def}_p(b) = 0$ which means

$$p(b-1, b+1) = 1 + (\text{the number of arcs in } \Theta(t) \text{ ending at } b^{\mathrm{I}}) = (*)$$

by Definition 5.4. There are two cases.

The first case is that b^{I} is strictly below an internal arc $\{a^{\mathrm{I}}, d^{\mathrm{I}}\} \in \Theta(t)$, whence $a < b < d$. Let P be the finite polygon below $\{a^{\mathrm{I}}, d^{\mathrm{I}}\}$. The restriction $\Theta(t)_P$ is a triangulation of P by Lemma 4.5. Since no arc in $\Theta(t)$ crosses $\{a^{\mathrm{I}}, d^{\mathrm{I}}\}$, we have

$$(*) = 1 + (\text{the number of arcs in } \Theta(t)_P \text{ ending at } b^{\mathrm{I}}) = (**).$$

The inclusion $\Theta(t) \subseteq \mathfrak{T}$ implies $\Theta(t)_P = \mathfrak{T}_P$ so we get the first of the following equalities,

$$\begin{aligned}(**) &= 1 + (\text{the number of arcs in } \mathfrak{T}_P \text{ ending at } b^{\mathrm{I}}) \\ &= 1 + (\text{the number of arcs in } \mathfrak{T} \text{ ending at } b^{\mathrm{I}}) = (***),\end{aligned}$$

where the second equality holds since $a < b < d$ and since no arc in $\mathfrak{T}$ crosses $\{a^{\mathrm{I}}, d^{\mathrm{I}}\} \in \mathfrak{T}$. Finally,

$$(***) = \mathfrak{T}\big((b-1)^{\mathrm{I}}, (b+1)^{\mathrm{I}}\big)$$

by Lemma 2.3(vi).

The second case is that b^{I} is strictly between the connecting arcs $\{a^{\mathrm{I}}, x^{\mathrm{III}}\}, \{d^{\mathrm{I}}, u^{\mathrm{III}}\} \in \Theta(t)$. This is handled similarly, replacing Lemma 4.5 by Lemma 4.7.

(ii) follows by symmetry. □

6. Case 1: SL_2-tilings with infinitely many entries equal to 1 in each of the first and third quadrants

Theorem 6.1. *Let t be an SL_2-tiling with infinitely many entries equal to 1 in each of the first and third quadrants.*

Consider D_2, the disc with two accumulation points and intervals denoted I *and* III*, see Figure 8.*

Then $\mathfrak{T} = \Theta(t)$ is a good triangulation of D_2 which satisfies $\Phi(\mathfrak{T}) = t$; see Figure 20.

Proof. Since t has infinitely many 1's in the first and the third quadrant, Lemma 3.9 implies that there are integers $\cdots < b_{-1} < b_0 < b_1 < \cdots$ and $\cdots < v_{-1} < v_0 < v_1 < \cdots$ such that $t(b_m, v_{-m}) = 1$ for each integer m. There are corresponding (connecting) arcs $\mathfrak{a}_m = \{b^{\mathrm{I}}_m, v^{\mathrm{III}}_{-m}\}$ in $\mathfrak{T} = \Theta(t)$. By Definition 1.10, the arcs $\mathfrak{a}_m$ can be viewed as dividing D_2 into finite polygons R_m, see Figure 20. For each m, Lemma 4.7 says that the arcs in $\mathfrak{T}$ between the vertices of R_m form a triangulation $\mathfrak{T}_{R_m}$ of R_m. It follows that the whole of $\mathfrak{T}$ is a triangulation

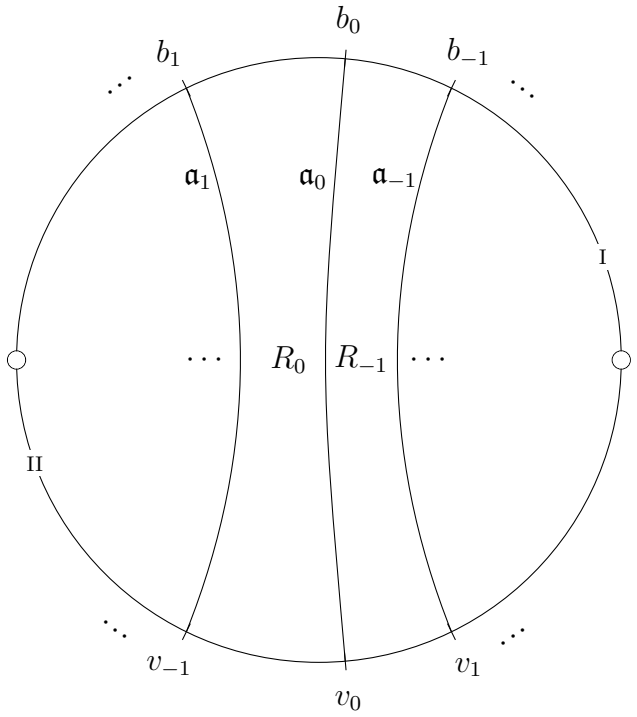

FIGURE 20. Outline of the triangulation $\mathfrak{T} = \Theta(t)$ of D_2 corresponding to an SL$_2$-tiling t with infinitely many entries equal to 1 in the first and the third quadrant, giving the connecting arcs $\mathfrak{a}_m$. Between the $\mathfrak{a}_m$ are the finite polygons R_m.

of D_2. The triangulation is good because the arcs $\mathfrak{a}_m$ block both accumulation points, see Definition 1.8.

To show $\Phi(\mathfrak{T}) = t$ we use Lemma 3.8:

Lemma 3.9 implies that there are integers $e < f$ and $g < h$ such that $t(e,h) = t(f,g) = t(f,h) = 1$. Hence the arcs $\{e^{\mathrm{I}}, h^{\mathrm{III}}\}$, $\{f^{\mathrm{I}}, g^{\mathrm{III}}\}$, $\{f^{\mathrm{I}}, h^{\mathrm{III}}\}$ are in $\mathfrak{T}$ whence $\mathfrak{T}(e^{\mathrm{I}}, h^{\mathrm{III}}) = \mathfrak{T}(f^{\mathrm{I}}, g^{\mathrm{III}}) = \mathfrak{T}(f^{\mathrm{I}}, h^{\mathrm{III}}) = 1$. This verifies condition (iii)' in Lemma 3.8.

The arcs $\mathfrak{a}_m$ mean that each vertex in intervals I and III is saturated. If b^{I} and v^{III} are given, Lemma 5.8 hence confirms conditions (i) and (ii) in Lemma 3.8. □

7. Case 2: SL$_2$-tilings with infinitely many entries equal to 1 only in the first or the third quadrant

By symmetry, it is enough to let t be an SL$_2$-tiling with infinitely many entries equal to 1 in the first quadrant, but not in the third quadrant.

Remark 7.1. Consider D_3, the disc with three accumulation points and intervals denoted I, II, and III as in the left part of Figure 9. We will construct a good triangulation $\mathfrak{T}$ of D_3 such that $\Phi(\mathfrak{T}) = t$. The overall structure of $\mathfrak{T}$ is shown in Figure 21.

Note that if t had infinitely many ones in the third quadrant, but not in the first quadrant, then we would instead use the disc with three accumulation points and intervals denoted I,

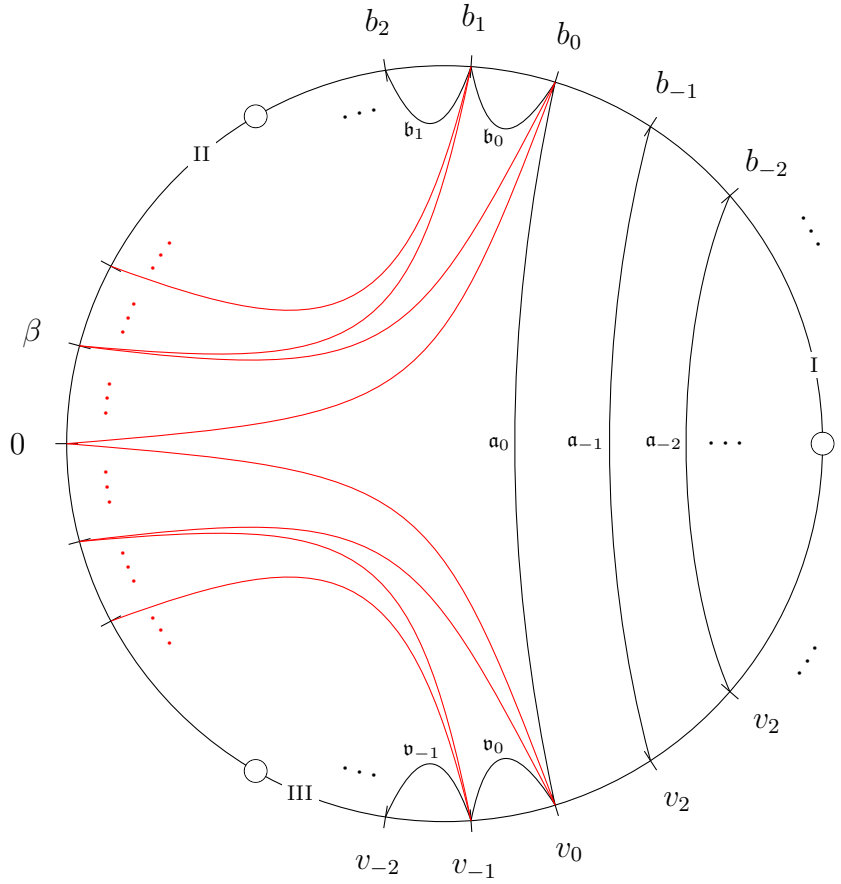

FIGURE 21. Outline of the triangulation $\mathfrak{T}$ of D_3 corresponding to an SL_2-tiling t with infinitely many entries equal to 1 only in the first quadrant. The arcs in $\Theta(t)$ are black. We add red arcs from the non-saturated vertices to define $\mathfrak{T}$. They connect each non-saturated vertex in intervals I and III to a block of consecutive vertices in interval II. The number of red arcs added at vertex b^{I} is $\mathrm{def}_p(b)$, and the number of red arcs added at vertex v^{III} is $\mathrm{def}_q(v)$.

III, and IV as in the right part of Figure 9. The overall structure of $\mathfrak{T}$ would be the mirror image in a vertical line of Figure 21.

Description 7.2 (The partial triangulation $\Theta(t)$)**.** The black arcs in Figure 21 show the overall structure of $\Theta(t)$ in D_3 which we now describe:

Using Lemma 3.9, we can suppose that among the entries in t which are equal to 1, the one which is furthest southwest is $t(b_0, v_0) = 1$. We can also choose integers $\cdots < b_{-1} < b_0$ and $v_0 < v_1 < \cdots$ such that $t(b_m, v_{-m}) = 1$ for $m \leqslant 0$. There are corresponding (connecting) arcs $\mathfrak{a}_m = \{b_m^{\mathrm{I}}, v_{-m}^{\mathrm{III}}\}$ in $\Theta(t)$.

The vertices $(b_0-1)^{\mathrm{I}}$, $(b_0-2)^{\mathrm{I}}$, ... and $(v_0+1)^{\mathrm{III}}$, $(v_0+2)^{\mathrm{III}}$, ... are saturated because of the arcs $\mathfrak{a}_m$. On the other hand, b_0^{I} is non-saturated: It is not strictly between two connecting arcs in $\Theta(t)$, nor is it strictly below an internal arc in $\Theta(t)$ because such an arc would have to cross $\{b_0^{\mathrm{I}}, v_0^{\mathrm{III}}\} \in \Theta(t)$.

Let $\mathfrak{b}_0 = \{b_0^{\mathrm{I}}, b_1^{\mathrm{I}}\}$ be either the longest internal arc in $\Theta(t)$ going anticlockwise from b_0^{I}, or, if there are no such arcs, the edge going anticlockwise from b_0^{I}. This makes sense because $\Theta(t)$ is locally finite by Lemma 4.4. It is easy to see that b_1^{I} is also non-saturated, while the vertices strictly below $\mathfrak{b}_0$ are saturated.

We can repeat this and thereby get integers $b_0 < b_1 < \cdots$ such that the non-saturated vertices in interval I are precisely b_0^{I}, b_1^{I}, ... A similar treatment provides integers $\cdots < v_{-1} < v_0$ such that the non-saturated vertices in interval III are precisely ..., v_{-1}^{III}, v_0^{III}.

Construction 7.3 (The triangulation $\mathfrak{T}$)**.** We add arcs to $\Theta(t)$ as follows to create a triangulation $\mathfrak{T}$ of D_3; see Figure 21 where the added arcs are shown in red:

From the non-saturated vertex b_0^{I}, add $\mathrm{def}_p(b_0)$ arcs ending at the consecutive vertices 0^{II}, -1^{II}, ..., β^{II} in interval II. Note that $\mathrm{def}_p(b_0) > 0$ by Lemma 5.7(ii). Then, from the non-saturated vertex b_1^{I}, add $\mathrm{def}_p(b_1)$ arcs ending at the next block of consecutive vertices β^{II}, $(\beta-1)^{\mathrm{II}}$, ... in interval II. Continue in the same way with the non-saturated vertices b_2^{I}, b_3^{I}, ...

Finally, add arcs by a similar recipe from the non-saturated vertices v_0^{III}, v_{-1}^{III}, ..., using def_q instead of def_p.

Theorem 7.4. *Let t be an* SL$_2$*-tiling with infinitely many entries equal to* 1 *only in the first or the third quadrant.*

Then there is a good triangulation $\mathfrak{T}$ of D_3 such that $\Phi(\mathfrak{T}) = t$.

Proof. As remarked at the start of the section, it is enough by symmetry to let t be an SL$_2$-tiling with infinitely many entries equal to 1 in the first quadrant, but not in the third quadrant. Let $\mathfrak{T}$ be as in Construction 7.3, see Figure 21.

Consider the finite polygons between the arcs $\mathfrak{a}_m$ and below the arcs $\mathfrak{b}_{-m}$ and $\mathfrak{v}_m$ shown in Figure 21, see Definition 1.10. In each such polygon, $\Theta(t)$ and hence $\mathfrak{T}$ restricts to a triangulation by Lemmas 4.5 through 4.7. The arcs added at the end of Construction 7.3 (red in Figure 21) clearly complete $\mathfrak{T}$ to a triangulation of D_3.

The arcs $\mathfrak{a}_m$ block the accumulation point between intervals I and III, see Definition 1.8. The arcs added at the end of Construction 7.3 block the accumulation points between interval II and the other intervals. Hence $\mathfrak{T}$ is a good triangulation of D_3.

To show $\Phi(\mathfrak{T}) = t$ we use Lemma 3.8:

Lemma 3.9 implies that there are integers $e < f$ and $g < h$ so that $t(e,h) = t(f,g) = t(f,h) = 1$. Hence the arcs $\{e^{\mathrm{I}}, h^{\mathrm{III}}\}$, $\{f^{\mathrm{I}}, g^{\mathrm{III}}\}$, $\{f^{\mathrm{I}}, h^{\mathrm{III}}\}$ are in $\mathfrak{T}$ whence $\mathfrak{T}(e^{\mathrm{I}}, h^{\mathrm{III}}) = \mathfrak{T}(f^{\mathrm{I}}, g^{\mathrm{III}}) = \mathfrak{T}(f^{\mathrm{I}}, h^{\mathrm{III}}) = 1$. This verifies condition (iii)' in Lemma 3.8.

To verify Lemma 3.8, condition (i), note that if b is given such that b^{I} is saturated, then the condition holds by Lemma 5.8(i). If b^{I} is non-saturated, then $b = b_m$ for some $m \geqslant 0$. Definition 5.4 gives

$$(\text{the number of arcs in } \Theta(t) \text{ ending at } b^{\mathrm{I}}) = p(b-1, b+1) - \mathrm{def}_p(b) - 1.$$

Compared to $\Theta(t)$, the triangulation $\mathfrak{T}$ has an additional $\mathrm{def}_p(b)$ arcs ending at b^{I} by Construction 7.3, so

$$(\text{the number of arcs in } \mathfrak{T} \text{ ending at } b^{\mathrm{I}}) = p(b-1, b+1) - 1.$$

On the other hand, $\mathfrak{T}$ is a good triangulation of D_3 so

$$(\text{the number of arcs in } \mathfrak{T} \text{ ending at } b^{\mathrm{I}}) = \mathfrak{T}\big((b-1)^{\mathrm{I}}, (b+1)^{\mathrm{I}}\big) - 1$$

by Lemma 2.3(vi). The last two equations imply $p(b-1, b+1) = \mathfrak{T}\big((b-1)^{\mathrm{I}}, (b+1)^{\mathrm{I}}\big)$, verifying Lemma 3.8, condition (i).

Lemma 3.8, condition (ii) is verified by symmetry. □

8. Case 3: SL_2-tilings with entries equal to 1 only in a proper rectangle

Let t be an SL_2-tiling with entries equal to 1 only in a proper rectangle. We do not permit all the entries equal to 1 to occur in a single row or a single column; these cases are handled separately in Section 9.

Construction 8.1 (The triangulation $\mathfrak{T}$)**.** To construct $\mathfrak{T}$, proceed similarly to Construction 7.3.

The difference is that there are now only finitely many connecting arcs between intervals I and III. There will consequently be non-saturated vertices at *both* ends of each of intervals I and III, so to go from $\Theta(t)$ to a triangulation $\mathfrak{T}$ we will need *two* intervals in addition to I and III. Hence $\mathfrak{T}$ will be a triangulation of D_4.

This is shown in Figure 22 where the black arcs show the overall structure of $\Theta(t)$ and the red arcs are added to $\Theta(t)$ in order to obtain $\mathfrak{T}$. At the vertex b^{I} we add $\mathrm{def}_p(b)$ red arcs. At the vertex v^{III} we add $\mathrm{def}_q(v)$ red arcs.

Theorem 8.2. *Let t be an SL_2-tiling with entries equal to 1 only in a proper rectangle. We do not permit all the entries equal to 1 to occur in a single row or a single column.*

Then there is a good triangulation $\mathfrak{T}$ of D_4 such that $\Phi(\mathfrak{T}) = t$.

Proof. Using $\mathfrak{T}$ from Construction 8.1 (see Figure 22) the proof is similar to the proof of Theorem 7.4. □

9. Case 4: SL_2-tilings with entries equal to 1 only in a single row or column

By symmetry, it is enough to let t be an SL_2-tiling with entries equal to 1 only in a single row. We do not permit t to have fewer than two entries equal to 1. The case of a unique entry equal to 1 is handled in Section 10. The case of no entries equal to 1 is handled in Section 13.

By Lemma 3.4, only finitely many entries of t are equal to 1. Let them be $t(b_0, v_1) = \cdots = t(b_0, v_j) = 1$ with $j \geqslant 2$.

Description 9.1 (The partial triangulation $\Theta(t)$)**.** The black arcs in Figure 23 show the overall structure of $\Theta(t)$ which we now describe:

The only connecting arcs in $\Theta(t)$ are $\mathfrak{a}_\ell = \{b_0^{\mathrm{I}}, v_\ell^{\mathrm{III}}\}$ for $\ell \in \{1, \ldots, j\}$. The vertices $(v_1+1)^{\mathrm{III}}$, $\ldots$, $(v_j-1)^{\mathrm{III}}$ strictly between $\mathfrak{a}_1$ and $\mathfrak{a}_j$ are saturated, see Definition 5.2.

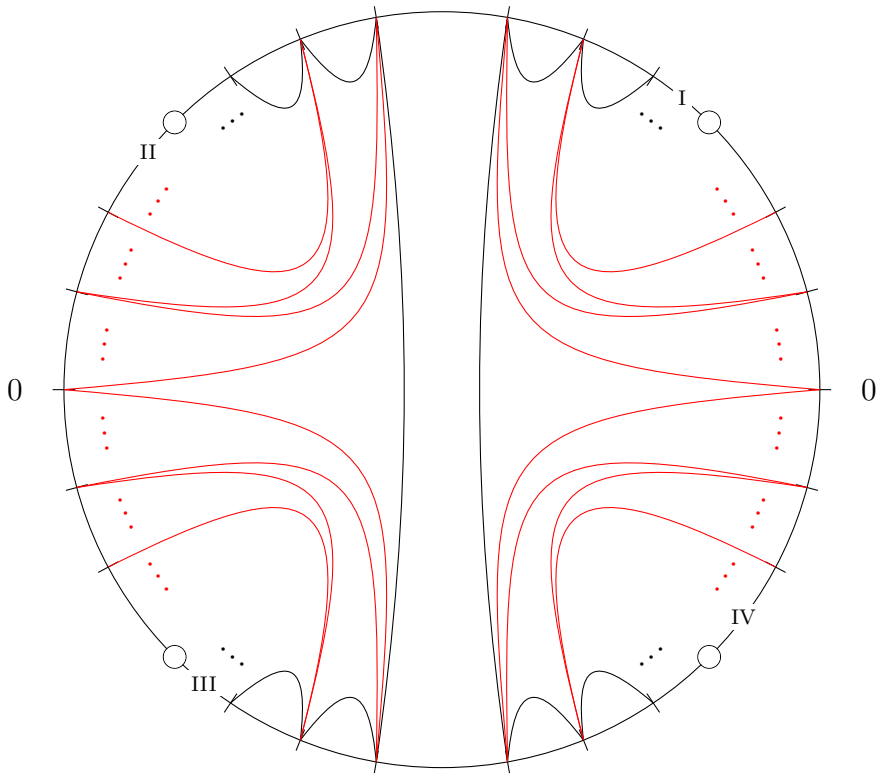

FIGURE 22. Outline of the triangulation $\mathfrak{T}$ of D_4 corresponding to an SL_2-tiling t with entries equal to 1 only in a proper rectangle. The arcs in $\Theta(t)$ are black. We add red arcs from the non-saturated vertices to define $\mathfrak{T}$. They connect each non-saturated vertex in intervals I and III to a block of consecutive vertices in interval II or IV. The number of red arcs added at the vertex b^{I} is $\mathrm{def}_p(b)$, and the number of red arcs added at the vertex v^{III} is $\mathrm{def}_q(v)$.

On the other hand, b_0^{I} is non-saturated: It is not strictly between two connecting arcs in $\Theta(t)$, nor is it strictly below an internal arc in $\Theta(t)$ because such an arc would have to cross $\{b_0^{\mathrm{I}}, v_1^{\mathrm{III}}\} \in \Theta(t)$. Similarly, v_1^{III} and v_j^{III} are non-saturated.

Let $\mathfrak{b}_0 = \{b_0^{\mathrm{I}}, b_1^{\mathrm{I}}\}$ be either the longest internal arc in $\Theta(t)$ going anticlockwise from b_0^{I}, or, if there are no such arcs, the edge going anticlockwise from b_0^{I}. This makes sense because $\Theta(t)$ is locally finite by Lemma 4.4. It is easy to see that b_1^{I} is also non-saturated, while the vertices strictly below $\mathfrak{b}_0$ are saturated.

We can repeat this to both sides of b_0 and thereby get integers $\cdots < b_{-1} < b_0 < b_1 < \cdots$ such that the non-saturated vertices in interval I are precisely the b_ℓ^{I}.

A similar treatment provides integers $\cdots < v_{-1} < v_0 < v_1$ and $v_j < v_{j+1} < v_{j+2} \cdots$ such that the non-saturated vertices in interval III are precisely $\ldots$, v_{-1}^{III}, v_0^{III}, v_1^{III} and v_j^{III}, v_{j+1}^{III}, v_{j+2}^{III}, $\ldots$.

Lemma 9.2. *With the notation of Description 9.1 and Figure 23, we have*

$$\mathrm{def}_p(b_0) - \big(t(b_{-1}, v_j) - 1\big) > 0.$$

Proof. We have

$$\mathrm{def}_p(b_0) - \big(t(b_{-1}, v_j) - 1\big) = t(b_1, v_1) - 1 > 0$$

where the equality is by Lemma 5.6 and the inequality is because $t(b_1, v_1) \neq 1$ by assumption. □

Construction 9.3 (The triangulation $\mathfrak{T}$)**.** We add arcs to $\Theta(t)$ as follows to create a triangulation $\mathfrak{T}$ of D_4; see Figure 23 where the added arcs are shown in red:

From vertex b_0^{I}, add $t(b_{-1}, v_j) - 1$ arcs ending at the consecutive vertices 0^{IV}, 1^{IV}, …, φ^{IV}. Note that $t(b_{-1}, v_j) - 1 > 0$ since $b_{-1} \neq b_0$.

From vertex b_{-1}^{I}, add $\mathrm{def}_p(b_{-1})$ arcs ending at the next block of consecutive vertices in interval IV. Note that $\mathrm{def}_p(b_{-1}) > 0$ by Lemma 5.7(ii). Continue in the same fashion with vertices b_{-2}^{I}, b_{-3}^{I}, ….

Going back to vertex b_0^{I}, add $\mathrm{def}_p(b_0) - \big(t(b_{-1}, v_j) - 1\big)$ arcs ending at the consecutive vertices 0^{II}, -1^{II}, …, β^{II}. This makes sense because $\mathrm{def}_p(b_0) - \big(t(b_{-1}, v_j) - 1\big) > 0$ by Lemma 9.2.

From vertex b_1^{I}, add $\mathrm{def}_p(b_1)$ arcs ending at the next block of consecutive vertices in interval II. Continue in the same fashion with vertices b_2^{I}, b_3^{I}, ….

Finally, add arcs by a similar recipe from vertices …, v_{-1}^{III}, v_0^{III}, v_1^{III} and v_j^{III}, v_{j+1}^{III}, v_{j+2}^{III}, … using def_q instead of def_p.

Theorem 9.4. *Let t be an SL_2-tiling with at least two entries equal to 1, and assume these occur only in a single row or in a single column.*

Then there is a good triangulation $\mathfrak{T}$ of D_4 such that $\Phi(\mathfrak{T}) = t$.

Proof. As remarked at the start of the section, it is enough by symmetry to let t be an SL_2-tiling with entries equal to 1 only in a single row. Let $\mathfrak{T}$ be as in Construction 9.3, see Figure 23.

Consider the finite polygons between the arcs $\mathfrak{a}_1$ and $\mathfrak{a}_j$ and below the arcs $\mathfrak{b}_m$ and $\mathfrak{v}_m$ shown in Figure 23, see Definition 5.1. In each such polygon, $\Theta(t)$ and hence $\mathfrak{T}$ restricts to a triangulation by Lemmas 4.5 through 4.7. The arcs added at the end of Construction 9.3 (red in Figure 23) clearly complete $\mathfrak{T}$ to a triangulation of D_4. These arcs also block all four accumulation points so $\mathfrak{T}$ is a good triangulation.

To show $\Phi(\mathfrak{T}) = t$ we use Lemma 3.8.

Since $\mathfrak{a}_1, \mathfrak{a}_j \in \mathfrak{T}$ we have

$$t(b_0, v_1) = 1 = \mathfrak{T}(b_0^{\mathrm{I}}, v_1^{\mathrm{III}}) \ , \ t(b_0, v_j) = 1 = \mathfrak{T}(b_0^{\mathrm{I}}, v_j^{\mathrm{III}}). \tag{9.1}$$

Moreover, the vertices b_{-1}^{I}, b_0^{I}, v_j^{III}, 0^{IV}, …, φ^{IV} can be viewed as the vertices of a finite polygon P inside which $\mathfrak{T}$ restricts to a triangulation $\mathfrak{T}_P$. In P, the vertices b_{-1}^{I}, b_0^{I}, v_j^{III}, are consecutive whence

$$\mathfrak{T}_P(b_{-1}^{\mathrm{I}}, v_j^{\mathrm{III}}) = 1 + (\text{the number of arcs in } \mathfrak{T}_P \text{ ending at } b_0^{\mathrm{I}}) = t(b_{-1}, v_j)$$

where the first equality is by Lemma 2.3(vi) and the second equality is by the construction of $\mathfrak{T}$, see Construction 9.3 and Figure 23. It follows that

$$t(b_{-1}, v_j) = \mathfrak{T}_P(b_{-1}^{\mathrm{I}}, v_j^{\mathrm{III}}) = \mathfrak{T}(b_{-1}^{\mathrm{I}}, v_j^{\mathrm{III}}), \tag{9.2}$$

where the second equality is by Remark 2.2. Equations (9.1) and (9.2) verify condition (iii)' in Lemma 3.8 with $e = b_{-1}$, $f = b_0$, $g = v_1$, $h = v_j$.

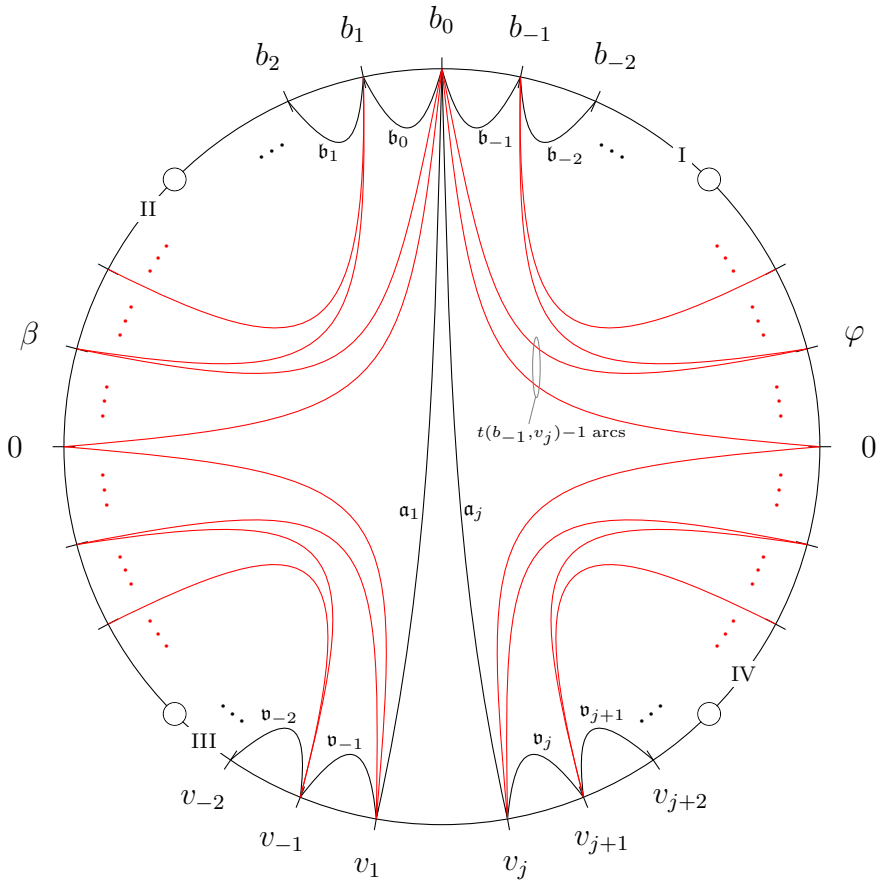

FIGURE 23. Outline of the triangulation $\mathfrak{T}$ of D_4 corresponding to an SL$_2$-tiling t with entries equal to 1 only in a single row. The arcs in $\Theta(t)$ are black. We add red arcs from the non-saturated vertices to define $\mathfrak{T}$. The number of red arcs added is given by the defect at the relevant vertex, but at b_0^{I} there is a choice of how many arcs should go to interval II, and how many to IV. This is resolved by letting $t(b_{-1}, v_j) - 1$ arcs go to IV.

Lemma 3.8, conditions (i) and (ii) are verified by the same method as in the last paragraph of the proof of Theorem 7.4. □

10. Case 5: SL$_2$-tilings with a unique entry equal to 1

Let t be an SL$_2$-tiling in which $t(b_0, v_1) = 1$ is the unique entry equal to 1.

Construction 10.1 (The triangulation $\mathfrak{T}$)**.** To construct $\mathfrak{T}$, proceed similarly to Construction 9.3 with a small tweak.

The black arcs in Figure 24 show the overall structure of $\Theta(t)$ which can be obtained by the method used in Description 9.1. However, there is now only a single connecting arc $\mathfrak{a} = \{b_0^{\mathrm{I}}, v_1^{\mathrm{III}}\}$.

When adding red arcs to obtain the triangulation $\mathfrak{T}$ of D_4, the red arcs go to interval II or interval IV, depending on which side of $\mathfrak{a}$ they are on. We always add as many red arcs at a vertex as dictated by the defect at that vertex.

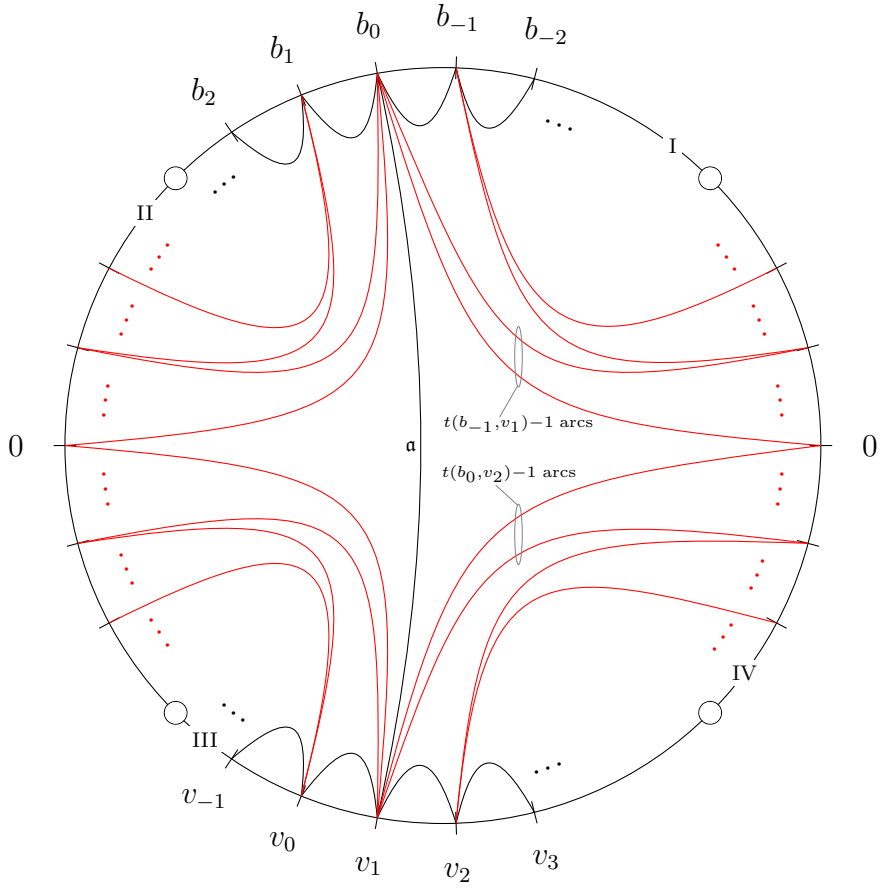

FIGURE 24. Outline of the triangulation $\mathfrak{T}$ of D_4 corresponding to an SL_2-tiling t with only a single entry equal to 1. The arcs in $\Theta(t)$ are black. We add red arcs from the non-saturated vertices to define $\mathfrak{T}$. The number of red arcs added is given by the defect at the relevant vertex, but at b_0^{I} there is a choice of how many arcs should go to interval II, and how many to IV. This is resolved by letting $t(b_{-1}, v_1) - 1$ arcs go to IV. Similarly at v_1^{III} we let $t(b_0, v_2) - 1$ arcs go to II.

At vertices b_0^{I} and v_1^{III} only, there are red arcs to both intervals II and IV.

From b_0^{I} there are $t(b_{-1}, v_1) - 1$ arcs to IV. Note that by Lemma 5.6, this number is strictly smaller than $\mathrm{def}_p(b_0)$, so there will also be at least one arc from b_0^{I} to II.

From v_1^{III} there are $t(b_0, v_2) - 1$ arcs to IV. Again, this number is strictly smaller than $\mathrm{def}_q(v_1)$, so there will also be at least one arc from v_1^{III} to II.

Theorem 10.2. *Let t be an SL_2-tiling with a unique entry equal to 1.*

Then there is a good triangulation $\mathfrak{T}$ of D_4 such that $\Phi(\mathfrak{T}) = t$.

Proof. We suppose $t(b_0, v_1) = 1$ and let $\mathfrak{T}$ be as in Construction 10.1, see Figure 24.

Arguing like the proof of Theorem 9.4, the choices at the end of Construction 10.1 imply that $\mathfrak{T}$ satisfies

$$t(b_{-1}, v_1) = \mathfrak{T}(b_{-1}^{\mathrm{I}}, v_1^{\mathrm{III}}) \ , \ t(b_0, v_2) = \mathfrak{T}(b_0^{\mathrm{I}}, v_2^{\mathrm{III}}).$$

We also have

$$t(b_0, v_1) = 1 = \mathfrak{T}(b_0^{\mathrm{I}}, v_1^{\mathrm{III}})$$

so condition (iii) of Lemma 3.8 holds with $e = b_{-1}$, $f = b_0$, $g = v_1$, $h = v_2$. Now proceed like the proof of Theorem 9.4. □

11. A lemma on Conway–Coxeter friezes

Definition 11.1. In this section we will write $\mathscr{S} = \left\{ \begin{pmatrix} i & j \\ k & \ell \end{pmatrix} \in \mathrm{SL}_2(\mathbb{Z}) \middle| i, j, k, \ell \geqslant 0 \right\}$.

The following lemma was proved in [6, thm. 6.2] and [8, lem. 4.1].

Lemma 11.2. *Each X in $\mathscr{S}$ can be obtained by starting with the 2×2 identity matrix E and performing a sequence of operations of the form: add one of the rows to the other row, or add one of the columns to the other column.*

Lemma 11.3. *Let r and m be coprime integers with $0 < r < m$. There exists $\begin{pmatrix} i & j \\ k & \ell \end{pmatrix}$ in $\mathscr{S}$ such that $r = i + j$, $m = i + j + k + \ell$.*

Proof. Set $n = m - r$. Then r and n are coprime so there are integers s, p with $sr - pn = 1$.

We can replace s, p with $s + tn$, $p + tr$ so may assume $0 \leqslant p < r$. It follows that $0 \leqslant pn < rn$, and since $pn = rs - 1$ this reads $0 \leqslant rs - 1 < rn$, that is $1 \leqslant rs < rn + 1$, that is $1 \leqslant rs \leqslant rn$. Hence $1 \leqslant s \leqslant n$.

It is now straightforward to check that

$$\begin{pmatrix} i & j \\ k & \ell \end{pmatrix} = \begin{pmatrix} r - p & p \\ n - s & s \end{pmatrix}$$

can be used in the lemma. □

Lemma 11.4. *Let r and m be coprime integers with $0 < r < m$.*

There exists a finite polygon R which has two adjacent vertices χ and $\chi^+ = \beta$, two adjacent vertices γ and $\gamma^+ = \varphi$, and a triangulation $\mathfrak{S}$ such that

$$r = \mathfrak{S}(\chi, \gamma) + \mathfrak{S}(\chi, \varphi),$$
$$m = \mathfrak{S}(\chi, \gamma) + \mathfrak{S}(\chi, \varphi) + \mathfrak{S}(\beta, \gamma) + \mathfrak{S}(\beta, \varphi).$$

Proof. By Lemma 11.3 there is

$$X = \begin{pmatrix} i & j \\ k & \ell \end{pmatrix}$$

in $\mathscr{S}$ with $r = i + j$, $m = i + j + k + \ell$. It is hence enough to show the following:

(a) There exists a finite polygon R which has two adjacent vertices χ and $\chi^+ = \beta$, two adjacent vertices γ and $\gamma^+ = \varphi$, and a triangulation $\mathfrak{S}$ such that X is equal to

$$Y = \begin{pmatrix} \mathfrak{S}(\chi, \gamma) & \mathfrak{S}(\chi, \varphi) \\ \mathfrak{S}(\beta, \gamma) & \mathfrak{S}(\beta, \varphi) \end{pmatrix}. \tag{11.1}$$

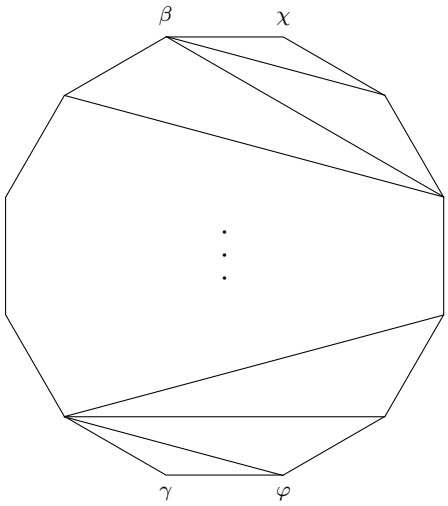

FIGURE 25. The polygon R with two adjacent vertices χ, β, two adjacent vertices γ, φ, and a triangulation $\mathfrak{S}$.

To show that (a) holds for each X in $\mathscr{S}$, it is enough to show the following by Lemma 11.2.

(i) If $X = E$ then (a) holds.

(ii) If (a) holds for a matrix X in $\mathscr{S}$, then it also holds for the matrices X' obtained from X by operations of the form: add one of the rows to the other row, or add one of the columns to the other column.

(i) is true since for $X = E$, we can let R be the 2-gon with $\chi = \varphi$ equal to one of the vertices, $\beta = \gamma$ equal to the other, and $\mathfrak{S}$ empty.

(ii): Suppose that (a) holds for X in $\mathscr{S}$ with the polygon R and triangulation $\mathfrak{S}$. Let Ψ denote one of the operations described in (ii) and perform Ψ on X to obtain a new matrix X'. To show that (a) holds for X', it is enough to show that there is a way to change R and $\mathfrak{S}$ to R' and $\mathfrak{S}'$ such that Ψ is performed on the matrix Y in equation (11.1).

We specialise to Ψ being the operation of adding the first row to the second, since the other operations have similar proofs. To go from R and $\mathfrak{S}$ to R' and $\mathfrak{S}'$, it turns out that we can glue an "ear" as illustrated by going from Figure 25 to Figure 26. That is, R' keeps the vertices of R, with β renamed β_{old}, and acquires a new vertex, β_{new}, between β_{old} and χ. And $\mathfrak{S}'$ keeps the arcs of $\mathfrak{S}$ and acquires a new arc, $\{\chi, \beta_{\text{old}}\}$.

It is clear from Definition 2.1 that for an arbitrary pair of the vertices χ, β_{old}, γ, φ in Figure 26, Conway–Coxeter counting on $\mathfrak{S}$ and $\mathfrak{S}'$ gives the same result. Hence the first row of Y is unchanged by going to R' and $\mathfrak{S}'$.

If γ is not equal to β_{old} or χ then the arcs $\{\beta_{\text{old}}, \chi\}$ and $\{\beta_{\text{new}}, \gamma\}$ in R' cross, so the Ptolemy formula in Lemma 2.3(v) gives

$$\mathfrak{S}'(\beta_{\text{old}}, \chi)\mathfrak{S}'(\beta_{\text{new}}, \gamma) = \mathfrak{S}'(\beta_{\text{old}}, \gamma)\mathfrak{S}'(\beta_{\text{new}}, \chi) + \mathfrak{S}'(\beta_{\text{old}}, \beta_{\text{new}})\mathfrak{S}'(\chi, \gamma).$$

Since $\{\beta_{\text{old}}, \chi\}$ is in $\mathfrak{S}'$ and $\{\beta_{\text{new}}, \chi\}$, $\{\beta_{\text{old}}, \beta_{\text{new}}\}$ are edges, the corresponding factors in the equation are equal to 1. This gives the first of the following equalities:

$$\mathfrak{S}'(\beta_{\text{new}}, \gamma) = \mathfrak{S}'(\beta_{\text{old}}, \gamma) + \mathfrak{S}'(\chi, \gamma) = \mathfrak{S}(\beta_{\text{old}}, \gamma) + \mathfrak{S}(\chi, \gamma).$$

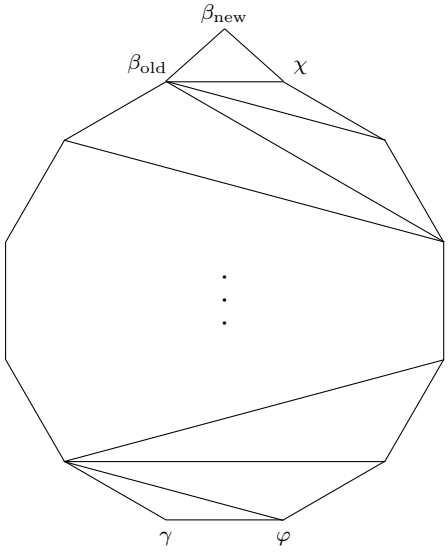

FIGURE 26. Compared to Figure 25, an "ear" has been glued to the triangulated polygon R, resulting in a new triangulated polygon R'.

This also holds trivially for γ equal to β_{old} or χ, and the same computation works with φ instead of γ. Hence the first row of Y is added to the second by going to R' and $\mathfrak{S}'$. □

12. An SL_2-tiling with no entry equal to 1 has a unique minimum

The following lemma is obvious.

Lemma 12.1. *Suppose that* $\begin{pmatrix} i & j \\ k & \ell \end{pmatrix}$ *is in* $\mathrm{SL}_2(\mathbb{Z})$ *and that each entry is* $\geqslant 1$. *If two entries which are horizontal or vertical neighbours are equal, then they are equal to* 1.

Lemma 12.2. *Suppose that* $\begin{pmatrix} i & j \\ k & \ell \end{pmatrix}$ *is in* $\mathrm{SL}_2(\mathbb{Z})$, *has each entry* $\geqslant 2$, *and that* $j < \ell$, $k < \ell$. *Then* $i < j$, $i < k$.

Proof. Lemma 12.1 implies that we cannot have $i = j$. If we had $i > j$ then we would have $i\ell > j\ell$. But we know $\ell > k$ whence $j\ell > jk$. Combining the inequalities would give $i\ell > j\ell > jk$ so the determinant of the matrix would be $i\ell - jk \geqslant 2$ which is false.

It follows that $i < j$, and $i < k$ is proved by considering the transpose. □

Lemma 12.3. *(i) If* $t(b, v)$ *is a local maximum in the* b*'th row of* t *in the sense that*

$$t(b, v-1) < t(b, v) > t(b, v+1), \tag{12.1}$$

then deleting the v*'th column from* t *gives a new* SL_2*-tiling.*

(ii) If $t(b, v)$ *is a local maximum in the* v*'th column of* t *in the sense that*

$$t(b-1, v) < t(b, v) > t(b+1, v),$$

then deleting the b*'th row from* t *gives a new* SL_2*-tiling.*

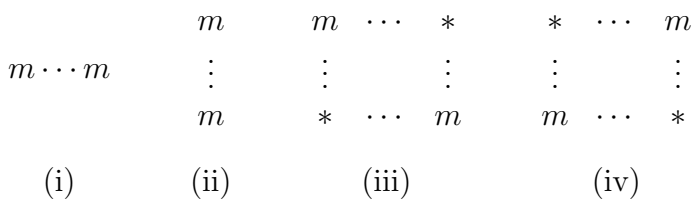

FIGURE 27. A minimal entry m appearing twice in an SL_2-tiling would have to do so in one of these patterns.

Proof. (i): The second Ptolemy relation of Lemma 3.3(ii) gives $q(v-1,v+1)t(c,v) = q(v-1,v)t(c,v+1) + q(v,v+1)t(c,v-1)$ for each c, that is

$$q(v-1,v+1)t(c,v) = t(c,v+1) + t(c,v-1).$$

Set $c = b$ and combine with the inequalities in part (i) of the lemma. It follows that the positive integer $q(v-1,v+1)$ must be 1, so the displayed equation reads

$$t(c,v) = t(c,v+1) + t(c,v-1)$$

for each c. It is elementary from this that deleting from t the v'th column with entries $t(-,v)$ gives a new SL_2-tiling.

(ii) follows by symmetry. □

Lemma 12.4. *Let t be an SL_2-tiling with no entry equal to 1. Then t has a unique minimal entry.*

Proof. If the minimal entry $m \geqslant 2$ occurred twice in t, then it would do so in one of the patterns shown in Figure 27. We treat the cases separately.

(i): Suppose that the b'th row of t has at least two entries equal to m. Pick two such entries which have no entries between them equal to m. Then either the two m's are neighbours, or each entry between them is $> m$.

In the latter case, somewhere between the two m's is a local maximum $t(b,v)$ in the sense of Equation (12.1). By Lemma 12.3(i), we can delete column number v and get a new SL_2-tiling. If we iterate this process, then all entries between the two m's will eventually be deleted, giving an SL_2-tiling where the two m's are neighbours.

However, two neighbouring m's would contradict Lemma 12.1.

(ii): Symmetric to (i), replacing Lemma 12.3(i) with Lemma 12.3(ii).

(iii): Suppose that the two entries equal to m are $t(b,v) = t(c,w) = m$ with $b < c$, $v < w$. Then the Ptolemy relation in Lemma 3.3(iii) implies

$$m^2 = t(b,w)t(c,v) + p(b,c)q(v,w).$$

However, this contradicts that $t(b,w), t(c,v) \geqslant m$ while $p(b,c), q(v,w) \geqslant 1$.

(iv): Suppose that the two entries equal to m are $t(b,v) = t(c,w) = m$ with $b > c$, $v < w$. Repeat as many times as possible the process of seeking out local maxima among the entries $t(b,v+1)$, …, $t(b,w-1)$ and $t(c,v+1)$, …, $t(c,w-1)$ and deleting the corresponding columns using Lemma 12.3(i). Then repeat as many times as possible the process of seeking

$$\begin{array}{ccccccccc}
* & > & * & > & \cdots & > & m \\
\vee & & & & & & \wedge \\
\vdots & & & & & & \vdots \\
\vee & & & & & & \wedge \\
* & & & & & & * \\
\vee & & & & & & \wedge \\
m & < & * & < & \cdots & < & *
\end{array}$$

FIGURE 28. If an SL_2-tiling t has no entries equal to 1 but has minimal entry m occurring twice in the pattern from Figure 27(iv), then we can achieve the inequalities shown here by deleting rows and columns from t.

out local maxima among the entries $t(c+1, v)$, ..., $t(b-1, v)$ and $t(c+1, w)$, ..., $t(b-1, w)$ and deleting the corresponding rows using Lemma 12.3(ii).

The resulting SL_2-tiling t' still contains the two entries equal to m which we started with, and they are still minimal. Since the local maxima are gone, the entries of t' satisfy the inequalities in Figure 28. Note that the inequalities are sharp by Lemma 12.1 because each entry of t' is $\geqslant 2$.

Starting from the lower right corner of Figure 28 and moving left using Lemma 12.2 repeatedly would give that the two lower rows of Figure 28 satisfied the following inequalities.

$$\begin{array}{ccccccc}
* & < & * & < & \cdots & < & * \\
\wedge & & & & & & \wedge \\
m & < & * & < & \cdots & < & *
\end{array}$$

However, the leftmost inequality contradicts Figure 28. □

13. CASE 6: SL_2-TILINGS WITH NO ENTRY EQUAL TO 1

Let t be an SL_2-tiling with no entry equal to 1 and unique minimal entry $t(b, v)$, see Lemma 12.4.

Notation 13.1. Let us describe part of what is shown with black arcs in Figure 29: Since $\Theta(t)$ is locally finite by Lemma 4.4, we can let $a < b < c$ be such that

- $\mathfrak{b}_{-1} = \{b^{\mathrm{I}}, a^{\mathrm{I}}\}$ is the longest internal arc in $\Theta(t)$ going clockwise from b^{I}, or, if there are no such arcs, the edge going clockwise from b^{I},
- $\mathfrak{b}_0 = \{b^{\mathrm{I}}, c^{\mathrm{I}}\}$ is the longest internal arc in $\Theta(t)$ going anticlockwise from b^{I}, or, if there are no such arcs, the edge going anticlockwise from b^{I}.

Likewise, we can let $v < w$ be such that

- $\mathfrak{v}_1 = \{v^{\mathrm{III}}, w^{\mathrm{III}}\}$ is the longest internal arc in $\Theta(t)$ going anticlockwise from v^{III}, or, if there are no such arcs, the edge going anticlockwise from v^{III}.

Lemma 13.2. *Consider the following divisions with remainders:*

$$t(a,v) = \ell t(b,v) + r, \quad 0 \leqslant r < t(b,v),$$
$$t(b,w) = mt(b,v) + s, \quad 0 \leqslant s < t(b,v).$$

Then

(i) $0 < \ell < \mathrm{def}_p(b)$,

(ii) $0 < m < \mathrm{def}_q(v)$,

(iii) $rs \equiv 1 \bmod t(b,v)$. *Note that since* $0 \leqslant r, s < t(b,v)$ *by definition, it follows that* $0 < r, s < t(b,v)$ *and that* r, s *are inverses modulo* $t(b,v)$.

Proof. (i): Since t has no entries equal to 1, there are no connecting arcs in $\Theta(t)$. In particular, $\Theta(t)$ has no connecting arcs ending at b^{I}, so Lemma 5.5 can be applied; see also Figure 18. In the lemma and the figure, we must set $b_{-1} = a$, $b_0 = b$, $b_1 = c$ to match the notation of this section. The lemma gives

$$p(a,c) = \mathrm{def}_p(b) + 1.$$

The Ptolemy relation in Lemma 3.3(ii) implies

$$p(a,c)t(b,v) = p(a,b)t(c,v) + p(b,c)t(a,v).$$

Here $p(a,b) = p(b,c) = 1$ since $\{a^{\mathrm{I}}, b^{\mathrm{I}}\}, \{b^{\mathrm{I}}, c^{\mathrm{I}}\} \in \Theta(t)$, so combining the displayed equations shows $\big(\mathrm{def}_p(b) + 1\big)t(b,v) = t(c,v) + t(a,v)$, that is,

$$t(a,v) = \big(\mathrm{def}_p(b) + 1\big)t(b,v) - t(c,v) < \mathrm{def}_p(b)t(b,v)$$

where the inequality holds since $t(b,v)$ is the unique minimal entry of t. This implies part (i).

(ii): Follows by symmetry.

(iii): The Ptolemy relation in Lemma 3.3(iii) implies

$$t(a,v)t(b,w) = t(a,w)t(b,v) + p(a,b)q(v,w).$$

Here $p(a,b) = q(v,w) = 1$ since $\{a^{\mathrm{I}}, b^{\mathrm{I}}\}, \{v^{\mathrm{III}}, w^{\mathrm{III}}\} \in \Theta(t)$ so

$$t(a,v)t(b,w) \equiv 1 \bmod t(b,v).$$

Since $t(a,v) \equiv r \bmod t(b,v)$ and $t(b,w) \equiv s \bmod t(b,v)$ by definition of r and s, part (iii) follows. □

Remark 13.3. Parts (i) and (ii) of the lemma imply $\mathrm{def}_p(b) \geqslant 2$ and $\mathrm{def}_q(v) \geqslant 2$ so b^{I} and v^{III} are non-saturated vertices by Lemma 5.7.

Description 13.4 (The partial triangulation $\Theta(t)$)**.** The black arcs in Figure 29 show the overall structure of $\Theta(t)$ which we now describe:

We will set $b_0 = b$ and $v_0 = v$. The vertex b_0^{I} is non-saturated by Remark 13.3. Let $\mathfrak{b}_0 = \{b_0^{\mathrm{I}}, b_1^{\mathrm{I}}\}$ be either the longest internal arc in $\Theta(t)$ going anticlockwise from b_0^{I}, or, if there are no such arcs, the edge going anticlockwise from b_0^{I}. This makes sense because $\Theta(t)$ is locally finite by Lemma 4.4. It is easy to see that b_1^{I} is also non-saturated, while the vertices strictly below $\mathfrak{b}_0$ are saturated.

We can repeat this to both sides of b_0 and thereby get integers $\cdots < b_{-1} < b_0 < b_1 < \cdots$ such that the non-saturated vertices in interval I are precisely $\ldots, b_{-1}^{\mathrm{I}}, b_0^{\mathrm{I}}, b_1^{\mathrm{I}}, \ldots$.

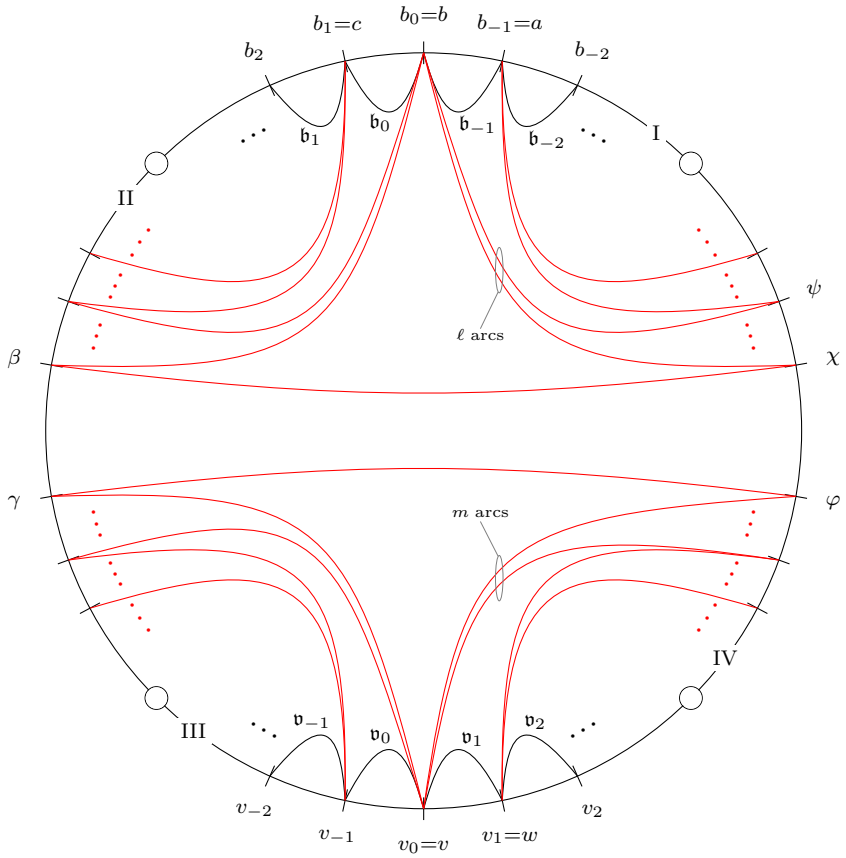

FIGURE 29. Outline of the triangulation $\mathfrak{T}$ of D_4 corresponding to an SL$_2$-tiling t with no entry equal to 1. The arcs in $\Theta(t)$ are black. We add red arcs from the non-saturated vertices to define $\mathfrak{T}$. The total number of red arcs added is given by the defect at the relevant vertex. The vertices b_0^{I} and v_0^{III} are the only ones with red arcs both to intervals II and IV. These vertices are chosen by $t(b_0, v_0)$ being the unique minimal entry in t.

A similar treatment provides integers $\cdots < v_{-1} < v_0 < v_1 < \cdots$ such that the non-saturated vertices in interval III are precisely $\ldots, v_{-1}^{\mathrm{III}}, v_0^{\mathrm{III}}, v_1^{\mathrm{III}}, \ldots$.

Note that we already considered some "longest arcs" in Notation 13.1, and that hence,

$$a = b_{-1}\ ,\ b = b_0\ ,\ c = b_1\ ,\ v = v_0\ ,\ w = v_1.$$

Construction 13.5 (The triangulation $\mathfrak{T}$)**.** We add arcs to $\Theta(t)$ as follows to create a triangulation $\mathfrak{T}$ of D_4; see Figure 29 where the added arcs are shown in red:

The vertices β^{II}, γ^{II}, φ^{IV}, χ^{IV} will be explained at the end; for the time being, consider them fixed and add the arcs $\{\chi^{\mathrm{IV}}, \beta^{\mathrm{II}}\}$ and $\{\gamma^{\mathrm{II}}, \varphi^{\mathrm{IV}}\}$.

Recall the numbers ℓ, m, and r from Lemma 13.2.

From vertex b_0^{I}, add ℓ arcs ending at the consecutive vertices χ^{IV}, $(\chi+1)^{\mathrm{IV}}$, …, ψ^{IV}. Also from vertex b_0^{I}, add $\mathrm{def}_p(b_0) - \ell$ arcs ending at the consecutive vertices β^{II}, $(\beta-1)^{\mathrm{II}}$, …. This makes sense because ℓ and $\mathrm{def}_p(b_0) - \ell$ are both positive by Lemma 13.2(i).

From vertex b_1^{I}, add $\mathrm{def}_p(b_1)$ arcs ending at the next block of consecutive vertices in interval II. Continue in the same fashion with vertices b_2^{I}, b_3^{I}, ….

From vertex b^{I}_{-1}, add $\mathrm{def}_p(b_{-1})$ arcs ending at the next block of consecutive vertices in interval IV. Continue in the same fashion with vertices b^{I}_{-2}, b^{I}_{-3}, ….

Add arcs by a similar recipe from the vertices $\cdots$, v^{III}_{-1}, v^{III}_{0}, v^{III}_{1}, $\cdots$ using m, def_q, γ^{II}, φ^{IV}, instead of ℓ, def_p, β^{II}, χ^{IV}.

Now consider the finite polygon R between the arcs $\{\chi^{\mathrm{IV}}, \beta^{\mathrm{II}}\}$ and $\{\gamma^{\mathrm{II}}, \varphi^{\mathrm{IV}}\}$. Viewed in R, each of χ^{IV}, β^{II} and γ^{II}, φ^{IV} is a pair of adjacent vertices. By Lemma 13.2(iii) we may apply Lemma 11.4, and thus, if we space each pair β^{II}, γ^{II} and φ^{IV}, χ^{IV} suitably, then there is a triangulation $\mathfrak{S}$ of R which satisfies

$$\begin{aligned} r &= \mathfrak{S}(\chi^{\mathrm{IV}}, \gamma^{\mathrm{II}}) + \mathfrak{S}(\chi^{\mathrm{IV}}, \varphi^{\mathrm{IV}}), \\ t(b, v) &= \mathfrak{S}(\chi^{\mathrm{IV}}, \gamma^{\mathrm{II}}) + \mathfrak{S}(\chi^{\mathrm{IV}}, \varphi^{\mathrm{IV}}) + \mathfrak{S}(\beta^{\mathrm{II}}, \gamma^{\mathrm{II}}) + \mathfrak{S}(\beta^{\mathrm{II}}, \varphi^{\mathrm{IV}}). \end{aligned} \tag{13.1}$$

The final step in constructing $\mathfrak{T}$ is to add to it the arcs in $\mathfrak{S}$.

Proposition 13.6. *The $\mathfrak{T}$ of Construction 13.5 is a good triangulation of D_4.*

Proof. Consider the finite polygons below the arcs $\mathfrak{b}_j$ and $\mathfrak{v}_j$ shown in Figure 29. In each such polygon, $\Theta(t)$ and hence $\mathfrak{T}$ restricts to a triangulation by Lemmas 4.5 through 4.7. The arcs added in Construction 13.5 (red in Figure 29) clearly complete $\mathfrak{T}$ to a triangulation of D_4. The added arcs also block the accumulation points of D_4 so $\mathfrak{T}$ is a good triangulation. □

The following lemma collects several consequences of the Ptolemy relation in Lemma 2.3(v) applied to $\mathfrak{T}$.

Lemma 13.7. *The numbers ℓ and m from Lemma 13.2 and the triangulation $\mathfrak{T}$ from Construction 13.5 satisfy the following.*

(i) *(a)* $\mathfrak{T}(a^{\mathrm{I}}, \beta^{\mathrm{II}}) = \ell + 1$.
(b) $\mathfrak{T}(w^{\mathrm{III}}, \gamma^{\mathrm{II}}) = m + 1$.

(ii) $\mathfrak{T}(\chi^{\mathrm{IV}}, v^{\mathrm{III}})\mathfrak{T}(\varphi^{\mathrm{IV}}, b^{\mathrm{I}}) \equiv 1 \bmod \mathfrak{T}(b^{\mathrm{I}}, v^{\mathrm{III}})$.

(iii) *(a)* $\mathfrak{T}(\chi^{\mathrm{IV}}, \gamma^{\mathrm{II}}) + \mathfrak{T}(\chi^{\mathrm{IV}}, \varphi^{\mathrm{IV}}) = \mathfrak{T}(\chi^{\mathrm{IV}}, v^{\mathrm{III}})$.
(b) $\mathfrak{T}(\varphi^{\mathrm{IV}}, \beta^{\mathrm{II}}) + \mathfrak{T}(\varphi^{\mathrm{IV}}, \chi^{\mathrm{IV}}) = \mathfrak{T}(\varphi^{\mathrm{IV}}, b^{\mathrm{I}})$.
(c) $\mathfrak{T}(\beta^{\mathrm{II}}, \gamma^{\mathrm{II}}) + \mathfrak{T}(\beta^{\mathrm{II}}, \varphi^{\mathrm{IV}}) = \mathfrak{T}(\beta^{\mathrm{II}}, v^{\mathrm{III}})$.

(iv) *(a)* $\mathfrak{T}(\beta^{\mathrm{II}}, v^{\mathrm{III}}) + \mathfrak{T}(\chi^{\mathrm{IV}}, v^{\mathrm{III}}) = \mathfrak{T}(b^{\mathrm{I}}, v^{\mathrm{III}})$.
(b) $\mathfrak{T}(\gamma^{\mathrm{II}}, b^{\mathrm{I}}) + \mathfrak{T}(\varphi^{\mathrm{IV}}, b^{\mathrm{I}}) = \mathfrak{T}(b^{\mathrm{I}}, v^{\mathrm{III}})$.

(v) $\mathfrak{T}(b^{\mathrm{I}}, v^{\mathrm{III}}) = \mathfrak{T}(\chi^{\mathrm{IV}}, \gamma^{\mathrm{II}}) + \mathfrak{T}(\chi^{\mathrm{IV}}, \varphi^{\mathrm{IV}}) + \mathfrak{T}(\beta^{\mathrm{II}}, \gamma^{\mathrm{II}}) + \mathfrak{T}(\beta^{\mathrm{II}}, \varphi^{\mathrm{IV}})$.

(vi) *(a)* $\big(\mathfrak{T}(a^{\mathrm{I}}, \beta^{\mathrm{II}}) - 1\big)\mathfrak{T}(b^{\mathrm{I}}, v^{\mathrm{III}}) + \mathfrak{T}(\chi^{\mathrm{IV}}, v^{\mathrm{III}}) = \mathfrak{T}(a^{\mathrm{I}}, v^{\mathrm{III}})$.
(b) $\big(\mathfrak{T}(w^{\mathrm{III}}, \gamma^{\mathrm{II}}) - 1\big)\mathfrak{T}(b^{\mathrm{I}}, v^{\mathrm{III}}) + \mathfrak{T}(\varphi^{\mathrm{IV}}, b^{\mathrm{I}}) = \mathfrak{T}(b^{\mathrm{I}}, w^{\mathrm{III}})$.

Proof. (i) Figure 29 shows that the vertex set $\{a^{\mathrm{I}}, b^{\mathrm{I}}, \beta^{\mathrm{II}}, \chi^{\mathrm{IV}}, \ldots, \psi^{\mathrm{IV}}\}$ is compatible with $\mathfrak{T}$ in the sense of Definition 1.10. These vertices span a finite polygon P and $\mathfrak{T}$ restricts to a triangulation $\mathfrak{T}_P$ of P. In P, the vertices a^{I}, b^{I}, β^{II} are consecutive, so Lemma 2.3(vi) gives

$$\mathfrak{T}_P(a^{\mathrm{I}}, \beta^{\mathrm{II}}) = 1 + (\text{the number of arcs in } \mathfrak{T}_P \text{ ending at } b^{\mathrm{I}}) = 1 + \ell.$$

By Remark 2.2 this implies part (i)(a), and part (i)(b) follows by symmetry.

(ii) If $\chi = \varphi$ then $\{\chi^{\mathrm{IV}}, v^{\mathrm{III}}\} = \{\varphi^{\mathrm{IV}}, v^{\mathrm{III}}\}$ and $\{\varphi^{\mathrm{IV}}, b^{\mathrm{I}}\} = \{\chi^{\mathrm{IV}}, b^{\mathrm{I}}\}$ are in $\mathfrak{T}$, so $\mathfrak{T}(\chi^{\mathrm{IV}}, v^{\mathrm{III}}) = \mathfrak{T}(\varphi^{\mathrm{IV}}, b^{\mathrm{I}}) = 1$ and part (ii) holds even without the congruence.

If $\chi \neq \varphi$ then the arcs $\{\chi^{\mathrm{IV}}, v^{\mathrm{III}}\}$ and $\{\varphi^{\mathrm{IV}}, b^{\mathrm{I}}\}$ cross so the Ptolemy relation gives

$$\begin{aligned}\mathfrak{T}(\chi^{\mathrm{IV}}, v^{\mathrm{III}})\mathfrak{T}(\varphi^{\mathrm{IV}}, b^{\mathrm{I}}) &= \mathfrak{T}(\chi^{\mathrm{IV}}, \varphi^{\mathrm{IV}})\mathfrak{T}(b^{\mathrm{I}}, v^{\mathrm{III}}) + \mathfrak{T}(\chi^{\mathrm{IV}}, b^{\mathrm{I}})\mathfrak{T}(\varphi^{\mathrm{IV}}, v^{\mathrm{III}}) \\ &\equiv \mathfrak{T}(\chi^{\mathrm{IV}}, b^{\mathrm{I}})\mathfrak{T}(\varphi^{\mathrm{IV}}, v^{\mathrm{III}}) \bmod \mathfrak{T}(b^{\mathrm{I}}, v^{\mathrm{III}}).\end{aligned}$$

This proves part (ii) because $\mathfrak{T}(\chi^{\mathrm{IV}}, b^{\mathrm{I}}) = \mathfrak{T}(\varphi^{\mathrm{IV}}, v^{\mathrm{III}}) = 1$ since $\{\chi^{\mathrm{IV}}, b^{\mathrm{I}}\}, \{\varphi^{\mathrm{IV}}, v^{\mathrm{III}}\} \in \mathfrak{T}$.

(iii) If $\chi = \varphi$ then part (iii)(a) claims

$$\mathfrak{T}(\varphi^{\mathrm{IV}}, \gamma^{\mathrm{II}}) + \mathfrak{T}(\chi^{\mathrm{IV}}, \chi^{\mathrm{IV}}) = \mathfrak{T}(\varphi^{\mathrm{IV}}, v^{\mathrm{III}}).$$

This equation just reads $1 + 0 = 1$ because $\{\varphi^{\mathrm{IV}}, \gamma^{\mathrm{II}}\}, \{\varphi^{\mathrm{IV}}, v^{\mathrm{III}}\} \in \mathfrak{T}$.

If $\chi \neq \varphi$ then the arcs $\{\chi^{\mathrm{IV}}, v^{\mathrm{III}}\}$ and $\{\gamma^{\mathrm{II}}, \varphi^{\mathrm{IV}}\}$ cross so the Ptolemy relation gives

$$\mathfrak{T}(\chi^{\mathrm{IV}}, v^{\mathrm{III}})\mathfrak{T}(\gamma^{\mathrm{II}}, \varphi^{\mathrm{IV}}) = \mathfrak{T}(\chi^{\mathrm{IV}}, \gamma^{\mathrm{II}})\mathfrak{T}(v^{\mathrm{III}}, \varphi^{\mathrm{IV}}) + \mathfrak{T}(\chi^{\mathrm{IV}}, \varphi^{\mathrm{IV}})\mathfrak{T}(v^{\mathrm{III}}, \gamma^{\mathrm{II}}).$$

This proves (iii)(a) because $\mathfrak{T}(\gamma^{\mathrm{II}}, \varphi^{\mathrm{IV}}) = \mathfrak{T}(v^{\mathrm{III}}, \varphi^{\mathrm{IV}}) = \mathfrak{T}(v^{\mathrm{III}}, \gamma^{\mathrm{II}}) = 1$ since $\{\gamma^{\mathrm{II}}, \varphi^{\mathrm{IV}}\}$, $\{v^{\mathrm{III}}, \varphi^{\mathrm{IV}}\}$, $\{v^{\mathrm{III}}, \gamma^{\mathrm{II}}\} \in \mathfrak{T}$. Parts (iii)(b) and (iii)(c) follow by symmetry.

(iv) The arcs $\{\beta^{\mathrm{II}}, \chi^{\mathrm{IV}}\}$ and $\{b^{\mathrm{I}}, v^{\mathrm{III}}\}$ cross so the Ptolemy relation gives

$$\mathfrak{T}(\beta^{\mathrm{II}}, \chi^{\mathrm{IV}})\mathfrak{T}(b^{\mathrm{I}}, v^{\mathrm{III}}) = \mathfrak{T}(\beta^{\mathrm{II}}, b^{\mathrm{I}})\mathfrak{T}(\chi^{\mathrm{IV}}, v^{\mathrm{III}}) + \mathfrak{T}(\beta^{\mathrm{II}}, v^{\mathrm{III}})\mathfrak{T}(\chi^{\mathrm{IV}}, b^{\mathrm{I}}).$$

This proves (iv)(a) because $\mathfrak{T}(\beta^{\mathrm{II}}, \chi^{\mathrm{IV}}) = \mathfrak{T}(\beta^{\mathrm{II}}, b^{\mathrm{I}}) = \mathfrak{T}(\chi^{\mathrm{IV}}, b^{\mathrm{I}}) = 1$ since $\{\beta^{\mathrm{II}}, \chi^{\mathrm{IV}}\}$, $\{\beta^{\mathrm{II}}, b^{\mathrm{I}}\}$, $\{\chi^{\mathrm{IV}}, b^{\mathrm{I}}\} \in \mathfrak{T}$. Part (iv)(b) is follows by symmetry.

(v) Combine parts (iii)(a), (iii)(c), and (iv)(a).

(vi) The arcs $\{a^{\mathrm{I}}, \beta^{\mathrm{II}}\}$ and $\{b^{\mathrm{I}}, v^{\mathrm{III}}\}$ cross so the Ptolemy relation gives

$$\mathfrak{T}(a^{\mathrm{I}}, \beta^{\mathrm{II}})\mathfrak{T}(b^{\mathrm{I}}, v^{\mathrm{III}}) = \mathfrak{T}(a^{\mathrm{I}}, b^{\mathrm{I}})\mathfrak{T}(\beta^{\mathrm{II}}, v^{\mathrm{III}}) + \mathfrak{T}(a^{\mathrm{I}}, v^{\mathrm{III}})\mathfrak{T}(\beta^{\mathrm{II}}, b^{\mathrm{I}}).$$

We have $\mathfrak{T}(a^{\mathrm{I}}, b^{\mathrm{I}}) = \mathfrak{T}(\beta^{\mathrm{II}}, b^{\mathrm{I}}) = 1$ since $\{a^{\mathrm{I}}, b^{\mathrm{I}}\}, \{\beta^{\mathrm{II}}, b^{\mathrm{I}}\} \in \mathfrak{T}$, so the equation reads

$$\mathfrak{T}(a^{\mathrm{I}}, \beta^{\mathrm{II}})\mathfrak{T}(b^{\mathrm{I}}, v^{\mathrm{III}}) = \mathfrak{T}(\beta^{\mathrm{II}}, v^{\mathrm{III}}) + \mathfrak{T}(a^{\mathrm{I}}, v^{\mathrm{III}}).$$

Combining with part (iv)(a) gives

$$\mathfrak{T}(a^{\mathrm{I}}, \beta^{\mathrm{II}})\mathfrak{T}(b^{\mathrm{I}}, v^{\mathrm{III}}) = \mathfrak{T}(b^{\mathrm{I}}, v^{\mathrm{III}}) - \mathfrak{T}(\chi^{\mathrm{IV}}, v^{\mathrm{III}}) + \mathfrak{T}(a^{\mathrm{I}}, v^{\mathrm{III}})$$

which can be reorganised into (vi)(a). Part (vi)(b) follows by symmetry. □

Theorem 13.8. *Let t be an SL_2-tiling with no entry equal to 1.*

Then there is a good triangulation $\mathfrak{T}$ of D_4 such that $\Phi(\mathfrak{T}) = t$.

Proof. Let $\mathfrak{T}$ be as in Construction 13.5, see Figure 29. It was proved in Proposition 13.6 that $\mathfrak{T}$ is a good triangulation of D_4. To show $\Phi(\mathfrak{T}) = t$ we use Lemma 3.8 in which we first verify condition (iii).

By construction, in the finite polygon R between the arcs $\{\chi^{\mathrm{IV}}, \beta^{\mathrm{II}}\}$ and $\{\gamma^{\mathrm{II}}, \varphi^{\mathrm{IV}}\}$, the triangulation $\mathfrak{T}$ agrees with the triangulation $\mathfrak{S}$ featured in Equations (13.1) which can hence be rewritten with $\mathfrak{T}$ instead of $\mathfrak{S}$. Combining with Lemma 13.7(iii)(a) gives

$$r = \mathfrak{T}(\chi^{\mathrm{IV}}, v^{\mathrm{III}}), \tag{13.2}$$

$$t(b, v) = \mathfrak{T}(\chi^{\mathrm{IV}}, \gamma^{\mathrm{II}}) + \mathfrak{T}(\chi^{\mathrm{IV}}, \varphi^{\mathrm{IV}}) + \mathfrak{T}(\beta^{\mathrm{II}}, \gamma^{\mathrm{II}}) + \mathfrak{T}(\beta^{\mathrm{II}}, \varphi^{\mathrm{IV}}). \tag{13.3}$$

Combining Equation (13.3) with Lemma 13.7(v) shows

$$t(b, v) = \mathfrak{T}(b^{\mathrm{I}}, v^{\mathrm{III}}). \tag{13.4}$$

Combining this with Lemma 13.2, Lemma 13.7(i)(a), and Equation (13.2) shows

$$t(a, v) = \ell t(b, v) + r = \big(\mathfrak{T}(a^{\mathrm{I}}, \beta^{\mathrm{II}}) - 1\big)\mathfrak{T}(b^{\mathrm{I}}, v^{\mathrm{III}}) + \mathfrak{T}(\chi^{\mathrm{IV}}, v^{\mathrm{III}}) = (*)$$

and Lemma 13.7(vi)(a) gives

$$(*) = \mathfrak{T}(a^{\mathrm{I}}, v^{\mathrm{III}}).$$

Now, on the one hand, Lemma 13.2(iii) says that $0 < r, s < t(b, v)$ and that r and s are inverses modulo $t(b, v)$. On the other hand, Lemma 13.7, (iii)(a), (iii)(b), and (v), imply that $0 < \mathfrak{T}(\chi^{\mathrm{IV}}, v^{\mathrm{III}}), \mathfrak{T}(\varphi^{\mathrm{IV}}, b^{\mathrm{I}}) < \mathfrak{T}(b^{\mathrm{I}}, v^{\mathrm{III}})$ and Lemma 13.7(ii) says that $\mathfrak{T}(\chi^{\mathrm{IV}}, v^{\mathrm{III}})$ and $\mathfrak{T}(\varphi^{\mathrm{IV}}, b^{\mathrm{I}})$ are inverses modulo $\mathfrak{T}(b^{\mathrm{I}}, v^{\mathrm{III}})$. Combining with Equations (13.2) and (13.4) shows $s = \mathfrak{T}(\varphi^{\mathrm{IV}}, b^{\mathrm{I}})$. We can now proceed as above, combining this with Lemma 13.2 and Lemma 13.7(i)(b) to get

$$t(b, w) = mt(b, v) + s = \big(\mathfrak{T}(w^{\mathrm{III}}, \gamma^{\mathrm{II}}) - 1\big)\mathfrak{T}(b^{\mathrm{I}}, v^{\mathrm{III}}) + \mathfrak{T}(\varphi^{\mathrm{IV}}, b^{\mathrm{I}}) = (**),$$

and Lemma 13.7(vi)(b) says

$$(**) = \mathfrak{T}(b^{\mathrm{I}}, w^{\mathrm{III}}).$$

Combining the last five displayed equations verifies Lemma 3.8, condition (iii), with $e = a$, $f = b$, $g = v$, $h = w$.

Finally, Lemma 3.8, conditions (i) and (ii) are verified by the same method as in the second half of the proof of Theorem 7.4. □

Acknowledgement. This work was carried out while Peter Jørgensen was visiting the Leibniz Universität Hannover. He thanks Thorsten Holm and the Institut für Algebra, Zahlentheorie und Diskrete Mathematik for their hospitality. He also gratefully acknowledges financial support from Thorsten Holm's grant HO 1880/5-1, which is part of the research priority programme SPP 1388 *Darstellungstheorie* of the Deutsche Forschungsgemeinschaft (DFG).

References

[1] I. Assem, G. Dupont, R. Schiffler, and D. Smith, *Friezes, strings and cluster variables*, Glasg. Math. J. **54** (2012), 27–60.
[2] I. Assem and C. Reutenauer, *Mutating seeds: types A and $\tilde{A}$*, Ann. Math. Blaise Pascal **19** (2012), 29–73.
[3] I. Assem, C. Reutenauer, and D. Smith, *Friezes*, Adv. Math. **225** (2010), 3134–3165.
[4] K. Baur, M. J. Parsons, and M. Tschabold, *Infinite friezes*, to appear in European J. Combin.
[5] F. Bergeron and C. Reutenauer, *SL_k-tilings of the plane*, Illinois J. Math. **54** (2010), 263–300.
[6] A. Blass and Y. Gurevich, *Matrix transformation is complete for the average case*, SIAM J. Comput. **24** (1995), 3–29.
[7] D. Broline, D. W. Crowe, and I. M. Isaacs, *The geometry of frieze patterns*, Geom. Dedicata **3** (1974), 171–176.
[8] J. Cai and J. Liu, *The bounded membership problem of the monoid $\mathrm{SL}_2(N)$*, Mathematical Systems Theory **29** (1996), 573–587.
[9] J. H. Conway and H. S. M. Coxeter, *Triangulated polygons and frieze patterns*, The Mathematical Gazette **57** (1973), 87–94.
[10] J. H. Conway and H. S. M. Coxeter, *Triangulated polygons and frieze patterns* (continued from p. 94), The Mathematical Gazette **57** (1973), 175–183.

[11] P. Di Francesco, *The non-commutative A_1 T-system and its positive Laurent property*, Comm. Math. Phys. **335** (2015), 935–953.
[12] P. Di Francesco, *The solution of the A_r T-system for arbitrary boundary*, Electron. J. Combin. **17** (2010), #R89.
[13] P. Di Francesco and R. Kedem, *T-systems with boundaries from network solutions*, Electron. J. Combin. **20** (2013), Paper 3, 62 pp.
[14] P. Di Francesco and R. Kedem, *The solution of the quantum A_1 T-system for arbitrary boundary*, Comm. Math. Phys. **313** (2012), 329–350.
[15] J. Grabowski and S. Gratz, *Cluster algebras of infinite rank*, with an appendix by M. Groechenig, J. London Math. Soc. (2) **89** (2014), 337–363.
[16] S. Gratz, T. Holm, and P. Jørgensen, Torsion pairs in infinite discrete cluster categories of Dynkin type A, in preparation.
[17] T. Holm and P. Jørgensen, *Generalised friezes and a modified Caldero-Chapoton map depending on a rigid object*, Nagoya Math. J. **218** (2015), 101–124.
[18] T. Holm and P. Jørgensen, *SL_2-tilings and triangulations of the strip*, J. Combin. Theory Ser. A **120** (2013), 1817–1834.
[19] K. Igusa and G. Todorov, *Cluster categories coming from cyclic posets*, Comm. Algebra **43** (2015), 4367–4402.
[20] P. Jørgensen and Y. Palu, *A Caldero-Chapoton map for infinite clusters*, Trans. Amer. Math. Soc. **365** (2013), 1125-1147.
[21] S. Morier-Genoud, *Coxeter's frieze patterns at the crossroads of algebra, geometry and combinatorics*, Bull. London Math. Soc. **47** (2015), 895–938.
[22] S. Morier-Genoud, V. Ovsienko, and S. Tabachnikov, *$\mathrm{SL}_2(\mathbb{Z})$-tilings of the torus, Coxeter-Conway friezes and Farey triangulations*, Enseign. Math. **61** (2015), 71–92.
[23] Y. Palu, *Cluster characters for 2-Calabi–Yau triangulated categories*, Ann. Inst. Fourier (Grenoble) **58** (2008), 2221–2248.
[24] M. Tschabold, *Arithmetic infinite friezes from punctured discs*, preprint (2015). `arXiv:1503.04352v3`.

Institut für Algebra, Zahlentheorie und Diskrete Mathematik, Fakultät für Mathematik und Physik, Leibniz Universität Hannover, Welfengarten 1, 30167 Hannover, Germany

E-mail address: `bessen@math.uni-hannover.de`

URL: `http://www2.iazd.uni-hannover.de/~bessen`

Institut für Algebra, Zahlentheorie und Diskrete Mathematik, Fakultät für Mathematik und Physik, Leibniz Universität Hannover, Welfengarten 1, 30167 Hannover, Germany

E-mail address: `holm@math.uni-hannover.de`

URL: `http://www.iazd.uni-hannover.de/~tholm`

School of Mathematics and Statistics, Newcastle University, Newcastle upon Tyne NE1 7RU, United Kingdom

E-mail address: `peter.jorgensen@ncl.ac.uk`

URL: `http://www.staff.ncl.ac.uk/peter.jorgensen`